Supporting Information

For

Ligand induced release of HNO/NO^- from a cobalt(II)-nitrosyl complex

Shankhadeep Saha,[a] Bristi Maina Deka,[a] Ankur K. Guha[b] and Biplab Mondal[*,a]*

[a]Department of Chemistry, Indian Institute of Technology Guwahati, Assam 781039, India. Phone: (+)91-361-2582317. Fax: (+)91-361-2582337. Email: biplab@iitg.ac.in.

[b]Department of Chemistry, Advanced Computational Chemistry Center, Cotton University, Guwahati, Assam -781001, India

Table of contents

Experimental Section

Materials and Methods

All experiments, unless otherwise specified, were done under argon atmosphere using standard Schlenk techniques on the Schlenk line. All chemicals used were of reagent grade, purchased from commercially available sources and no purification was done unless mentioned. Methanol was distilled using Mg-turnings and iodine. Dichloromethane was purified by passing through a basic alumina column, then storing it over calcium hydride overnight and followed by distillation under inert atmosphere (N_2). All the solvents were stored over molecular sieve (4 Å) for at least two days under argon before use. Molecular sieves were kept at 200 °C for 24 hours for activation and cooled under vacuum. In order to deoxygenate the solvents and solutions, vacuum/argon purge cycles were used repeatedly. All the reactions were performed under inert atmosphere except those mentioned differently. Agilent Cary 8454 spectrophotometer was applied to collect UV-visible spectra. A PerkinElmer spectrophotometer (Spectrum Two) was used to record FT-IR spectra of the samples using ATR probe. Bruker Avance III Varian FT-NMR spectrophotometers (400 and 500 MHz) were used for ^{1}H, ^{13}C, and ^{31}P-NMR studies. JES-FA200 EPR spectrophotometer was used to record

X-band EPR spectra (microwave frequency, 9.14 GHz; microwave power, 0.998 mW; and modulation amplitude, 2). Gas chromatograms were obtained on PerkinElmer Clarus® 590. Cyclic voltammetric studies were carried out on a Metrohm instrument MULTI AUTOLAB M204 machine with a cell having three electrode set-up. A platinum wire, a glassy carbon electrode and an $Ag/AgNO_3$ as working, counter and reference electrode, respectively. The complexes in dichloromethane containing 0.1 M $[(^{n}Bu)_4N]PF_6$ as supporting electrolyte were used.

Single crystals were grown from dichloromethane-methanol solutions using the slow evaporation technique. The X-ray diffraction data were recorded using a Bruker SMART APEX-II CCD diffractometer [Mo Kα radiation (λ = 0.71073 Å)]. The intensity data were collected with increasing ω (width of 0.3° per frame) at 3 s/frame scan speed. The SMART software was used for data acquisition. SAINT and XPREP software were used for data integration and reduction.[1] Structures were solved by direct methods using SHELXL[2a] and refined with full-matrix least-squares on F^2 (SHELXL-2019/1).[2b] Structural illustrations were drawn with ORTEP-3 for Windows.[2c] Non-hydrogen atoms were refined anisotropically.

Computational Details

Shapes and eigen values of the highest occupied molecular orbital (HOMO) and lowest unoccupied molecular orbital (LUMO) of complex **1a** was calculated at M06-2X/def2-TZVP level[3] from the crystallographic coordinates. Imidazole bound six coordinated intermediate was fully optimized at M06-2X/def2-TZVP level and harmonic vibrational frequency calculation reveals it to be a true minimum on the potential energy surface with all real values of the Hessian matrix. All these calculations were performed using GAUSSIAN 16 suite of program.[4]

Syntheses

5,7,12,14-tetramethyldibenzotetraaza[14]annulene (H_2TMTAA): The ligand is prepared following a reported procedure.[5] Briefly, the mixture of 1,2-phenylenediamine (8.92 g, 0.082 mol), 2,4-pentanedione (8.5 mL, 0.085 mol) and $Ni(OAc)_2.4H_2O$ (5 g, 0.02 mol) was refluxed in 125 mL n-butanol for 3 hours in a 250 mL round bottom flask. The reaction mixture was brought to room temperature and 50 mL methanol was added. Keeping this reaction mixture in an ice-bath for 30 minutes results in the formation of crystalline purple-blue solid which was collected by filtration. This purple-blue solid is identified as $[Ni^{II}(TMTAA^{2-})]$ complex.

Yield: 6.53 g (*ca.* 80%). Following that, methanolic (100 mL) solution of $[Ni^{II}(TMTAA^{2-})]$ (5 g, 0.012 mol) was prepared in an Erlenmeyer flask and HCl gas was bubbled through the solution. The solution became very hot and the color of the solution changed from green to brown. The solution was cooled to room temperature and a white precipitate formed. The precipitate is filtered off and washed with cold methanol. This white solid is identified as H_2TMTAA.2HCl. Yield: 4.35 g (*ca.* 84%). Then, a slurry of H_2TMTAA.2HCl (4.17 g, 0.010 mol) was prepared with 10 mL methanol in a 50 mL beaker. NEt_3 was added to it dropwise and the color of the slurry became yellow. When the pH of the mixture became 9, a bright yellow precipitate was formed. It was filtered, washed several times with cold methanol several times and air dried. H_2TMTAA was isolated as a yellow solid. Yield: 2.95 g (*ca.* 86%) Elemental analyses for $C_{22}H_{24}N_4$; Calculated (%): C, 76.71; H, 7.02; N, 16.27. Found (%): C, 76.79; H, 7.07; N, 16.41. FT-IR (in ATR probe): 1610, 1548, 1505, 1460, 1425, 1379, 1353, 1272, 1184, 1109, 1018, 802, 732 and 694 cm^{-1}. ^{1}H-NMR (400 MHz, $CDCl_3$): δ_{ppm}, 12.58 (s, 2H), 6.99 (s, 8H), 4.88 (s, 2H) and 2.13 (s, 12H). ^{13}C-NMR (100 MHz, $CDCl_3$): δ_{ppm}, 158.9, 138.5, 130.5, 123.1, 122.9, 97.9 and 20.9. ESI-mass (m/z): Calculated, 344.200; Found, 345.209 ($[M+H]^+$).

[$Co^{II}(TMTAA^{2-})$], 1: To a 25 mL round bottom flask equipped with a stir bar, dichloromethane (2 mL) solution of H_2TMTAA (68.8 mg, 0.2 mmol) and methanolic (5 mL) solution of $Co(OAc)_2.4H_2O$ (49.8 mg, 0.2 mmol) was added. The reaction mixture was stirred for 2 hours under argon atmosphere which resulted in precipitation. The brown precipitate was filtered off and washed several times with cold methanol. Complex **1** was isolated as a dark brown solid. Single crystals of complex **1** were obtained by layering a methanolic solution of $Co(OAc)_2.4H_2O$ over a dichloromethane solution of H_2TMTAA.

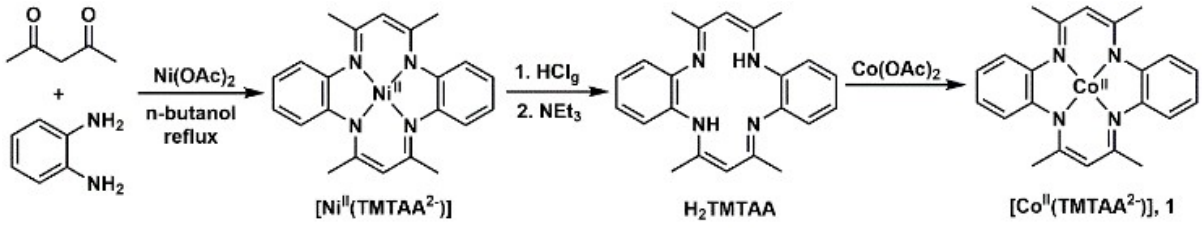

Scheme 1. Synthesis of H_2TMTAA ligand and precursor complex **1**.

Yield: 62 mg (*ca.* 77%) Elemental analyses for $C_{22}H_{22}N_4Co$; Calculated (%): C, 65.83; H, 5.52; N, 13.96. Found (%): C, 65.78; H, 5.57; N, 14.03. FT-IR (in ATR probe): 1579, 1532, 1517, 1461, 1432, 1388, 1362, 1274, 1199, 1032, 921, 777, 738 and 535 cm^{-1}. UV-visible (CH_2Cl_2): 367 nm ($\varepsilon/M^{-1}\ cm^{-1}$, 7.79×10^4), 415 nm ($\varepsilon/M^{-1}\ cm^{-1}$, 3.35×10^4), 460 nm ($\varepsilon/M^{-1}\ cm^{-1}$, 1.89×10^4), 533 nm ($\varepsilon/M^{-1}\ cm^{-1}$, 9.52×10^3) and 582 nm ($\varepsilon/M^{-1}\ cm^{-1}$, 9.57×10^3). ESI-mass (m/z): Calculated, 401.117; Found, 402.124 ($[M+H]^+$ peak). Crystal data: complex **1**, $C_{44}H_{44}Co_2N_8$, M = 802.73, Monoclinic ($P2_1/c$), a = 14.4344(8) Å, b = 16.4066(5) Å, c = 16.2778(7) Å, α = 90°, β = 99.840(4)°, γ = 90°, V = 3798.2(3) $Å^3$, Z = 4, D_c = 1.404 g cm^{-3}, μ = 0.917 mm^{-1}, T = 293(2) K, 14351 reflections, 6684 independent, $R(F)$ = 0.0453 [$I > 2\delta(I)$], R(int) = 0.0659, $wR(F2)$ = 0.1034 (all data), GOF = 0.998.

[Co(TMTAA^{2-})(NO)], 1a: Complex **1** (40 mg, 0.1 mmol), was dissolved in dry and degassed dichloromethane (4 mL) solution in a 25 mL round bottom flask equipped with a rubber septum and degassed thoroughly using argon/vacuum cycle. NO gas was purged through this solution for 2 minutes which resulted in a change in color of the solution from brown to dark-red. After standing at room temperature for 30 minutes, excess NO gas was removed by argon flush. Addition of dry and degassed methanol (10 mL) to this solution resulted in precipitation. Complex **1a** was isolated as a dark-red solid. The single crystals were obtained by slow evaporation of the dichloromethane solution. Yield: 36 mg (*ca.* 84%) Elemental analyses for $C_{23}H_{24}N_5OCl_2Co$; Calculated (%): C, 53.51; H, 4.69; N, 13.56. Found (%): C, 53.46; H, 4.74; N, 13.59. FT-IR (in ATR probe): 2963, 1622 (ν_{NO}), 1578, 1531, 1461, 1391, 1260, 1201, 1089, 1022, 798, 736 and 531 cm^{-1}. UV-visible (CH_2Cl_2): 337 nm (ε/M^{-1} cm^{-1}, 2.75 × 10^4), 399 nm (ε/M^{-1} cm^{-1}, 3.15 × 10^4) and 531 nm (ε/M^{-1} cm^{-1}, 8.62 × 10^3). ^{1}H-NMR (400 MHz, $CDCl_3$): δ_{ppm}, 7.13-7.09 (3, 4H), 6.95-6.90 (3, 4H), 4.55 (s, 2H) and 2.23 (s, 12H). Crystal data: **1a**, CCDC No. 2374826. $C_{23}Cl_2CoN_5OH_{24}$, M = 516.30, Triclinic (P -1), a = 9.1802(8) Å, b = 11.2850(10) Å, c = 12.0488(10) Å, α = 102.415(3)°, β = 94.370(3)°, γ = 104.862(3)°, V = 1166.81(18) Å^3, Z = 2, D_c = 1.470 g cm^{-3}, μ = 0.990 mm^{-1}, T = 296.0 K, 27316 reflections, 4111 independent, $R(F)$ = 0.0702 [$I > 2\delta(I)$], R(int) = 0.0728, $wR(F2)$ = 0.1832 (all data), GOF = 1.095.

^{15}NO-Labeled Complex 1a: Complex 1 (10 mg, 0.025 mmol) was dissolved in dry, degassed dichloromethane (2 mL) in a 25 mL round-bottom flask fitted with a rubber septum. The solution was thoroughly degassed by several argon/vacuum cycles. Subsequently, ^{15}NO gas was bubbled through the solution for approximately 2 min, leading to a color change from brown to dark red. The reaction mixture was then allowed to stand at room temperature for 30 min. Excess NO gas was removed by purging the solution with argon. Addition of dry, degassed methanol (10 mL) to the reaction mixture resulted in the formation of a precipitate.

The resulting dark-red solid (complex 1a) was isolated and characterized by IR spectroscopy. FT-IR (in ATR probe): 3044, 1590 (ν^{15}_{NO}), 1555, 1479, 1395, 1252, 1089, 1033, 799, 754 and 505 cm^{-1}.

[Co^{III}(TMTAA^{2-})(IM)](BPh$_4$), 2: Complex **1a** (43 mg, 0.1 mmol) was taken in a 15 mL Schlenk tube and degassed by consecutive argon/vacuum cycles. Dry and degassed dichloromethane was added to it resulting in a dark-red solution. Addition of imidazole (10 mg, 0.16 mmol) to this solution caused an immediate color change from red to orange-red. After keeping this reaction mixture at room temperature for 1 hour, methanolic solution of $NaBPh_4$ (68 mg, 0.2 mmol) was added and the reaction mixture was left overnight. Brown precipitation of complex **2** was observed which was collected by filtration followed by air drying. Yield: 66 mg (*ca.* 85%) Elemental analyses for $C_{49}H_{46}N_6BCo$; Calculated (%): C, 74.62; H, 5.88; N, 10.66. Found (%): C,74.57; H, 5.93; N, 10.71. FT-IR (in ATR probe): 3121, 2921, 2851, 1548, 1459, 1400, 1326, 1256, 1206, 1093, 1062, 1035, 930, 825, 744, 662 and 619 cm^{-1}. UV-visible (CH_2Cl_2): 355 nm ($\varepsilon/M^{-1}\ cm^{-1}$, 2.24×10^3), 447 nm ($\varepsilon/M^{-1}\ cm^{-1}$, 3.18×10^3) and 535 nm ($\varepsilon/M^{-1}\ cm^{-1}$, 1.12×10^3). ESI-mass (m/z): Calculated, 469.155; Found, 469.155 ([Co(TMTAA^{2-})(IM)]$^+$).

Reaction of complex 1a with imidazole: Complex **1a** (21 mg, 0.05 mmol) and imidazole (4 mg, 0.06 mmol) were taken in a reaction tube equipped with a magnetic stirring bar and degassed properly *via* consecutive argon/vacuum cycle. Dry and degassed dichloromethane (3 mL) was added to it and the reaction mixture was stirred at room temperature. The reaction progress was monitored using various spectroscopic techniques (UV-visible and FT-IR).

[Mn^{III}(TPP^{2-})Cl]: The complex was prepared using earlier reported procedure.[6a] Elemental analyses for $C_{44}H_{28}N_4ClMn$; Calculated (%): C, 75.16; H, 4.01; N, 7.97. Found (%): C, 75.20; H, 4.07; N, 8.02. FT-IR (in ATR probe): 2961, 1596, 1531, 1487, 1440, 1415, 1391, 1342,

1259, 1202, 1071, 1009, 797, 750, 700, 665 and 453 cm^{-1}. UV-visible (CH_2Cl_2): 475 nm (ε/M^{-1} cm^{-1}, 6.6×10^4), 579 nm (ε/M^{-1} cm^{-1}, 7.6×10^3) and 615 nm (ε/M^{-1} cm^{-1}, 7.6×10^3). ESI-mass (m/z): Calculated, 667.169; Found, 667.178 (For $[Mn(TPP^{2-})]^+$ unit).

$[Fe^{III}(TPP^{2-})Cl]$: The complex was prepared using earlier reported procedure.[6b] Elemental analyses for $C_{44}H_{28}N_4ClFe$; Calculated (%): C, 75.07; H, 4.01; N, 7.96. Found (%): C, 75.02; H, 3.95; N, 8.01. UV-visible (CH_2Cl_2): 416 nm (ε/M^{-1} cm^{-1}, 1.32×10^5), 509 nm (ε/M^{-1} cm^{-1}, 1.30×10^4), 570 nm (ε/M^{-1} cm^{-1}, 5.26×10^3) and 690 nm (ε/M^{-1} cm^{-1}, 1.91×10^3). FT-IR (in KBr): 1596, 1485, 1439, 1333, 1199, 1174, 1069, 1001, 994, 803, 747, and 701 cm^{-1}. ESI-mass (m/z): Calculated, 668.166; Found, 668.166 (For $[Fe(TPP^{2-})]^+$ unit).

Reaction of complex 1a with $[Mn^{III}(TPP^{2-})Cl]$ in the presence of imidazole: Complex **1a** (43 mg, 0.1 mmol), $[Mn^{III}(TPP^{2-})Cl]$ (70 mg, 0.1 mmol) and imidazole (8 mg, 0.12 mmol) was taken in a Schlenk tube and degassed it properly with argon flush. Dry and degassed dichloromethane (5 mL) was added to it and made the complexes soluble by stirring. $HBF_4.Et_2O$ (16 μL, 0.1 mmol) was added to the reaction mixture while stirring and monitored the progress of reaction using spectroscopic techniques. The $[Mn(TPP^{2-})(NO)]$ complex was isolated and characterized spectroscopically.

$[Mn(TPP^{2-})(NO)]$: Yield: 58 mg (*ca.* 83%). Elemental analyses for $C_{44}H_{28}N_5OFe$; Calculated (%): C, 75.75; H, 4.05; N, 10.04. Found (%): C, 75.81; H, 4.09; N, 9.95. FT-IR (in ATR probe): 2948, 1760 (ν_{NO}), 1594, 1536, 1486, 1439, 1347, 1261, 1203, 1174, 1068, 1000, 797, 752, 703 and 663 cm^{-1}. UV-visible (CH_2Cl_2): 429 nm (ε/M^{-1} cm^{-1}, 8.91×10^4), 548 nm (ε/M^{-1} cm^{-1}, 1.04×10^3) and 584 nm (ε/M^{-1} cm^{-1}, 5.81×10^3). ESI-mass (m/z): Calculated, 668.177; Found, 668.165 (after loss of NO, protonated).

Reaction of complex 1a with $[Fe^{III}(TPP^{2-})Cl]$ in presence of imidazole: Complex **1a** (43 mg, 0.1 mmol), $[Fe^{III}(TPP^{2-})Cl]$ (70 mg, 0.1 mmol) and imidazole (8 mg, 0.12 mmol) was taken

in a Schlenk tube and degassed it properly with argon flash. Dry and degassed dichloromethane (5 mL) was added to it and made the complexes soluble by stirring. $HBF_4.Et_2O$ (16 μL, 0.1 mmol) was added to the reaction mixture while stirring and monitor the progress of reaction using spectroscopic techniques. The [Fe(TPP^{2-})(NO)] complex was isolated and characterized spectroscopically.

[Fe(TPP^{2-})(NO)]: Yield: 56 mg (*ca.* 80%). Elemental analyses for $C_{44}H_{28}N_5OFe$; Calculated (%): C, 75.65; H, 4.04; N, 10.03. Found (%): C, 75.73; H, 4.13; N, 9.96. FT-IR (in ATR probe): 2917, 1695 (ν_{NO}), 1596, 1440, 1345, 1263, 1202, 1171, 1158, 1071, 1001, 995, 801, 751, 717, 702, 664 and 530 cm^{-1}. UV-visible (CH_2Cl_2): 412 nm ($\varepsilon/M^{-1}\ cm^{-1}$, 3.12×10^4), 540 nm ($\varepsilon/M^{-1}\ cm^{-1}$, 2.28×10^3) and 611 nm ($\varepsilon/M^{-1}\ cm^{-1}$, 8.17×10^2). ESI-mass (m/z): Calculated, 668.166; Found, 668.172 (after loss of NO).

Determination of the yield of N_2O: N-hydroxybenzenesulfonamide was taken in five 50 mL round-bottom flasks equipped with rubber septum in different measured amounts and degassed using argon/vacuum purge. 10 mL of 0.1 M NaOH solution was added to each flask under the sealed condition, and the reaction was allowed to proceed for 30 minutes. 1 mL of headspace gas from each reaction vessel was subjected to GC. From there, a calibration curve of the concentration of *N*-hydroxybenzenesulfonamide and peak area at 2.77 minutes (corresponding to N_2O) was drawn.

Complex **1a** (0.08 g, 0.2 mmol) and imidazole (0.02 g, 0.3 mmol) were dissolved in 10 mL of dry and degassed dichloromethane (5 mL) in a 50 mL round-bottom flask. 32 μL of $HBF_4 \cdot Et_2O$ was added to it after 5 minutes under anaerobic condition. The reaction was allowed to procced for 1 hour. After the completion of the reaction, 1 mL of headspace gas was subjected to GC. From the calibration curve, the amount of N_2O was measured. Yield: *ca.* 65% (0.13 mmol).

Reaction of complex 1a with morpholine: Complex **1a** (43 mg, 0.1 mmol) and morpholine (10 mg, 0.12 mmol) were placed in a Schlenk fask containing a magnetic stirring bar. The system was carefully degassed through several argon/vacuum cycles. Subsequently, dry and degassed dichloromethane (3 mL) was added, and the mixture was stirred at room temperature. The reaction was monitored by recording IR spectra at different time intervals. The IR data show that the characteristic ν(NO) band at 1622 cm^{-1} progressively decreases as the reaction proceeds, suggesting the loss of the coordinated nitrosyl group. Importantly, no new bands corresponding to nitrite or nitrate species were detected during the course of the reaction.

Reaction of complex 1a with [$Mn^{III}(TPP^{2-})Cl$] in the presence of morpholine: A trapping experiment was carried out using the well-known HNO trapping agent [$Mn^{III}(TPP^{2-})Cl$]. In this experiment, complex 1a (43 mg, 0.1 mmol), [$Mn^{III}(TPP^{2-})Cl$] (70 mg, 0.1 mmol), and morpholine (10 mg, 0.12 mmol) were placed in a round-bottom flask and the system was thoroughly degassed by argon flushing. Dry and degassed dichloromethane (5 mL) was then added, and the mixture was stirred until all components were completely dissolved. Subsequently, $HBF_4 \cdot Et_2O$ (16 µL, 0.1 mmol) was introduced into the reaction mixture under stirring. The progress of the reaction was monitored by IR spectroscopy.

The IR spectrum recorded after 1 h shows that the ν(NO) band at 1622 cm^{-1}, corresponding to complex 1a, is almost completely diminished. At the same time, a new band appears at 1755 cm^{-1}, which is characteristic of the formation of Mn(TPP)(NO).

Preparation of sample for ^{31}P-NMR spectroscopy: Complex **1a** (8.6 mg, 0.02 mmol), imidazole (1.5 mg, 0.025 mmol) and PPh_3 (10.4 mg, 0.04 mmol) were taken in an NMR tube and degassed thoroughly using continuous argon purge. Dry and degassed dichloromethane (0.3 mL) was added to it followed by HBF_4 (diluted in dichloromethane) and kept it at room

temperature for 2 hours. 0.1 mL of DMSO-d_6 was added to it and the reaction mixture was subjected to ^{31}P-NMR spectrophotometer.

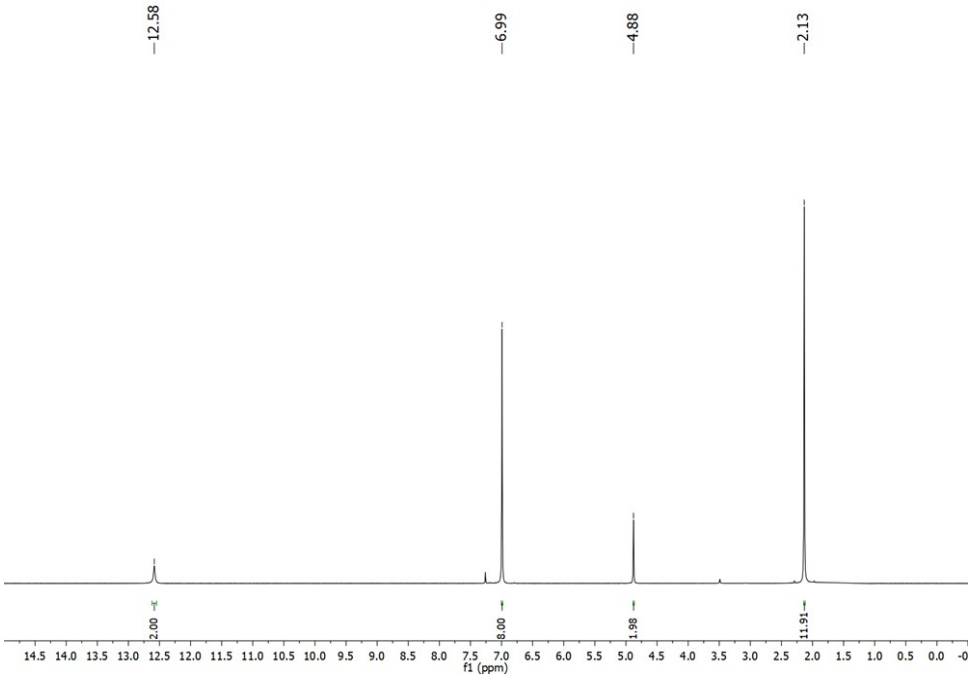

Figure S1. ^{1}H-NMR spectrum of **H_2TMTAA** in $CDCl_3$.

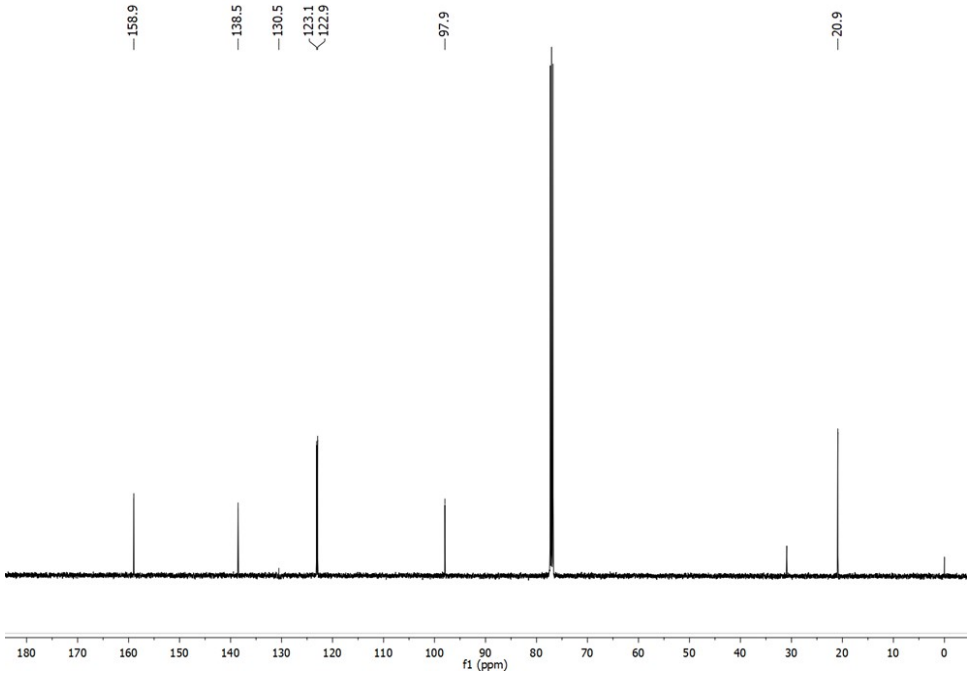

Figure S2. ^{13}C-NMR spectrum of **H_2TMTAA** in $CDCl_3$.

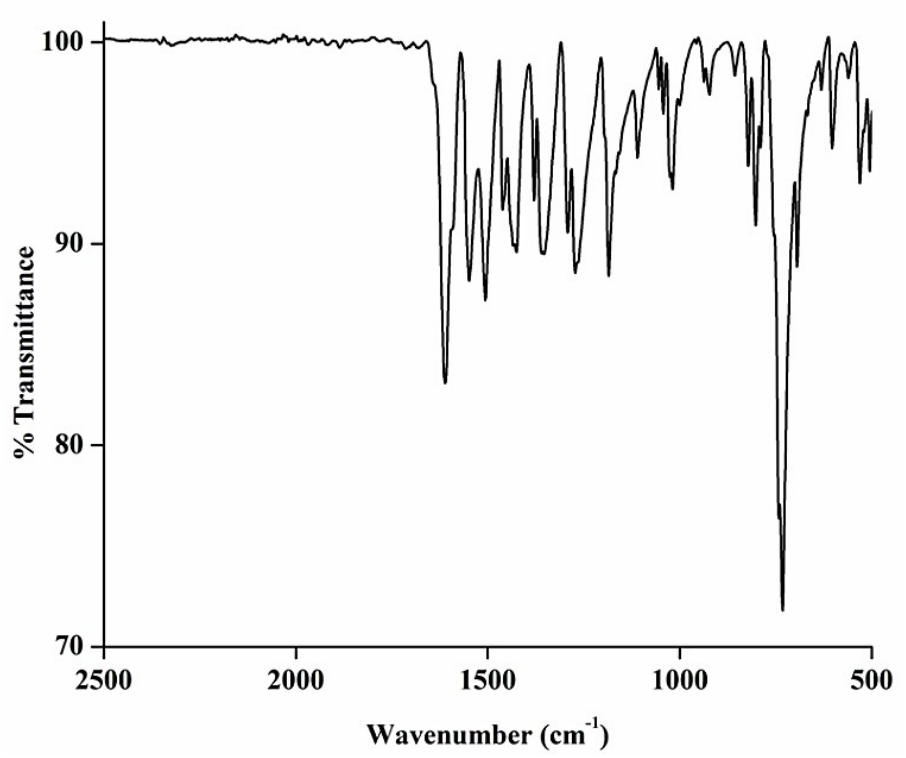

Figure S3. FT-IR spectrum of **H_2TMTAA** in ATR probe**.**

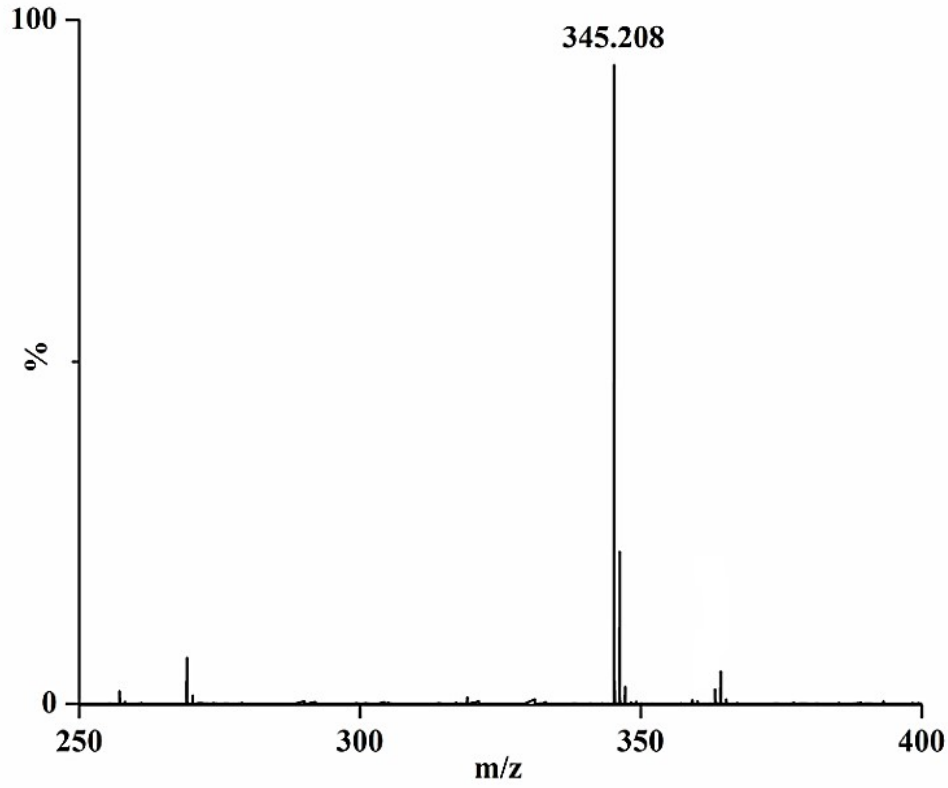

Figure S4. ESI-mass spectrum of **H_2TMTAA** in CH_3CN. **(**Calculated, 345.208; Found, 345.208, for $[M+H]^+$).

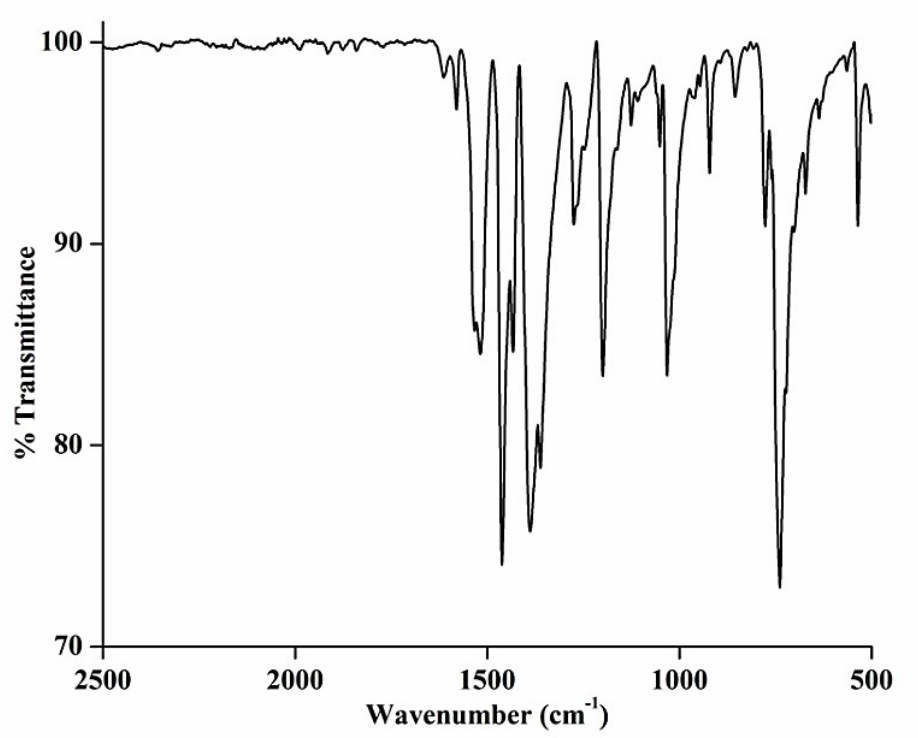

Figure S5. FT-IR spectrum of complex **1** in ATR probe.

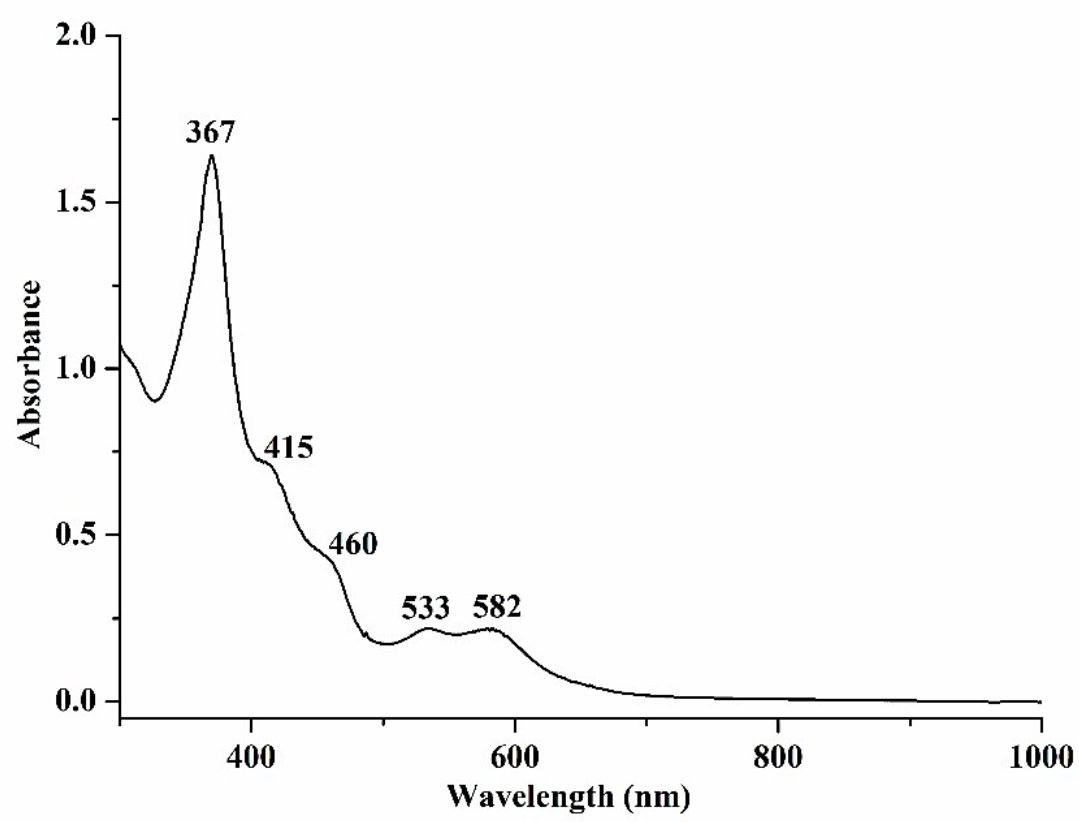

Figure S6. UV-visible spectrum of complex **1** in CH_2Cl_2 at room temperature.

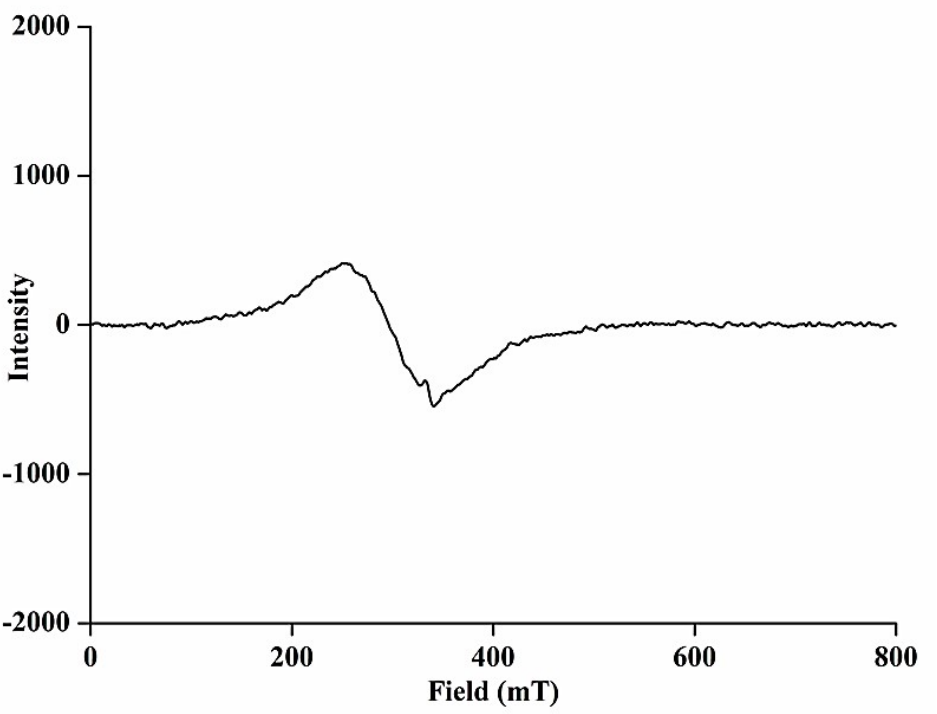

Figure S7. X-band EPR spectrum of complex **1** in CH_2Cl_2 at 77 K.

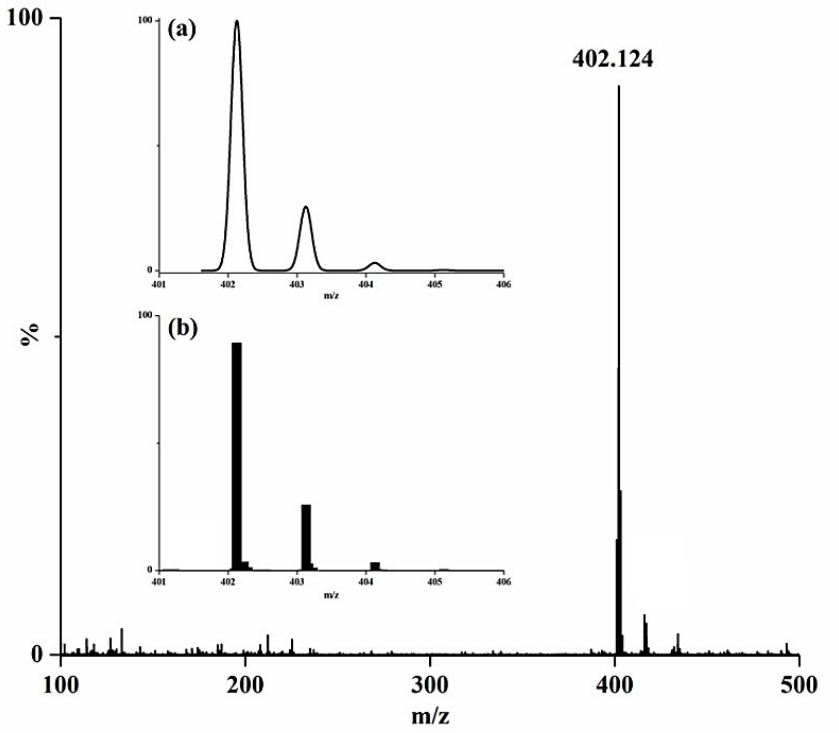

Figure S8. ESI-mass spectrum of complex **1** in CH_3CN **(**Calculated, 402.125; Found, 402.124; for $[M+H]^+$. Inset: Isotopic distribution pattern; (a) Simulated, (b) Experimental).

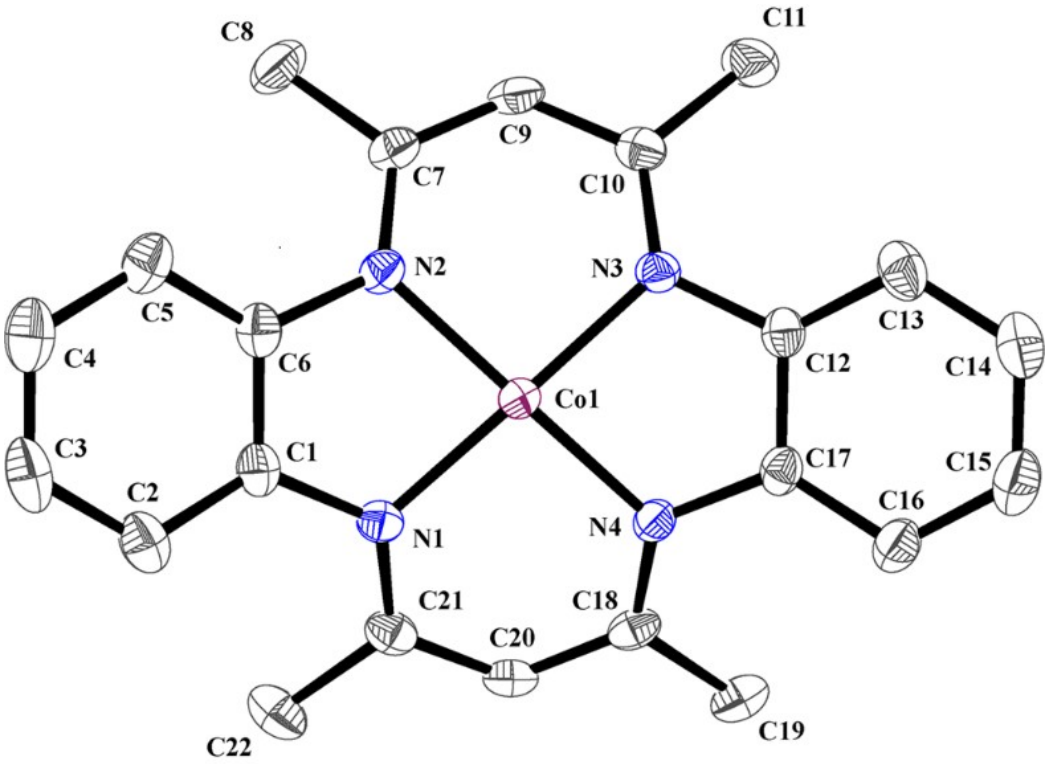

Figure S9. ORTEP diagram of complex **1 (**30% thermal ellipsoid. H atoms are omitted for clarity).

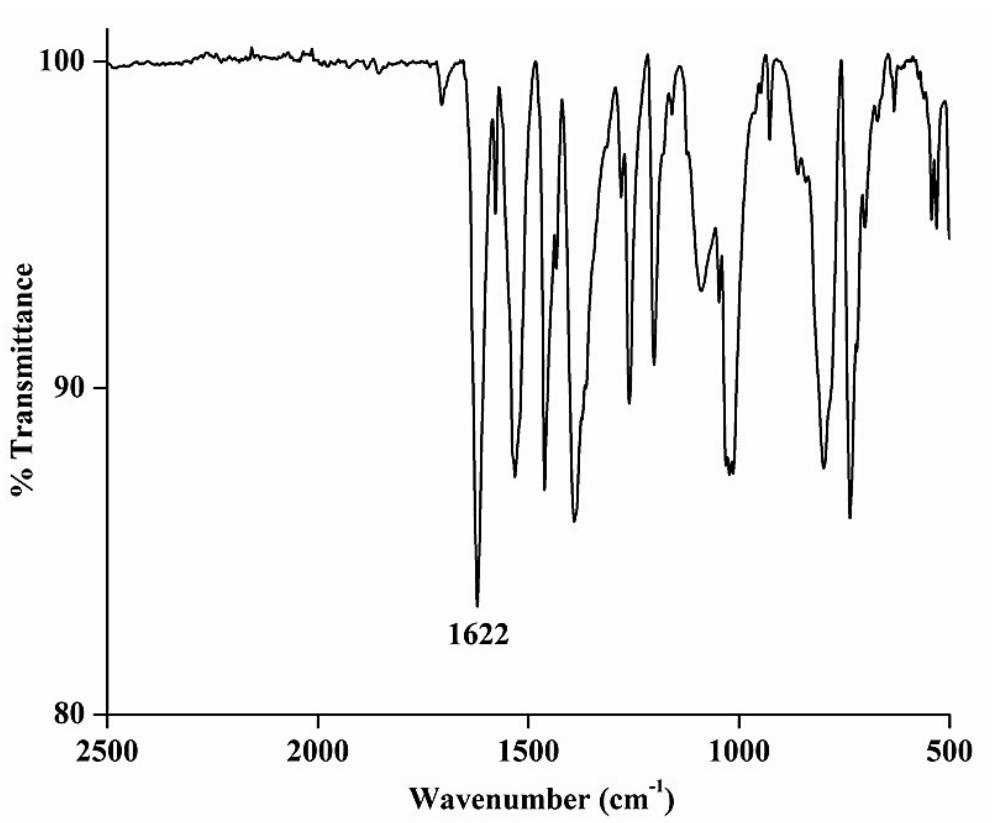

Figure S10a. FT-IR spectrum of complex **1a** in ATR probe.

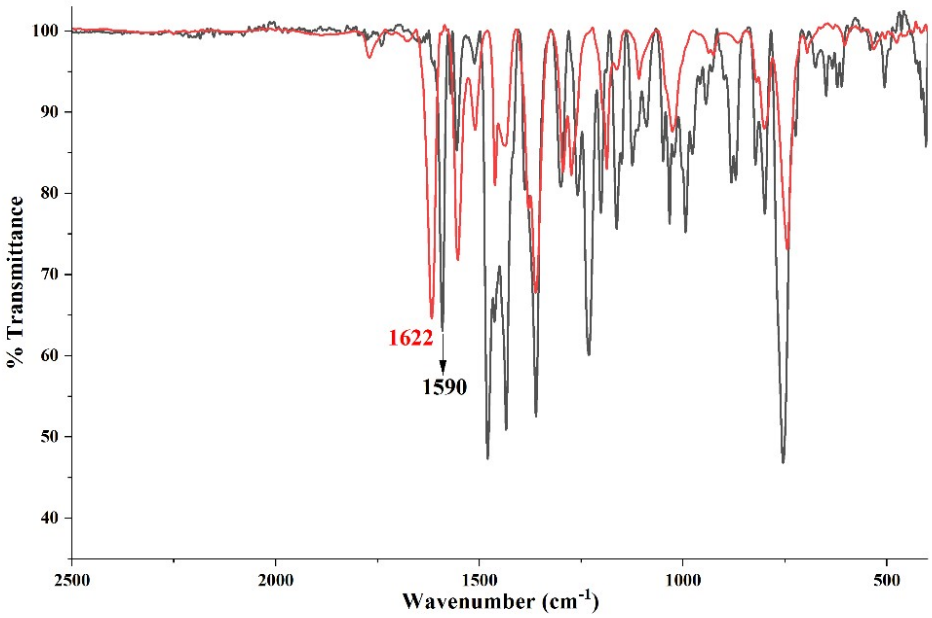

Figure S10b. FT-IR spectra of [Co(TMTAA)(NO)] showing isotopic substitution of NO. ^{14}NO complex (red) exhibits a υ(NO) band at 1622 cm^{-1}, which shifts to 1590 cm^{-1} upon ^{15}NO labelling (black).

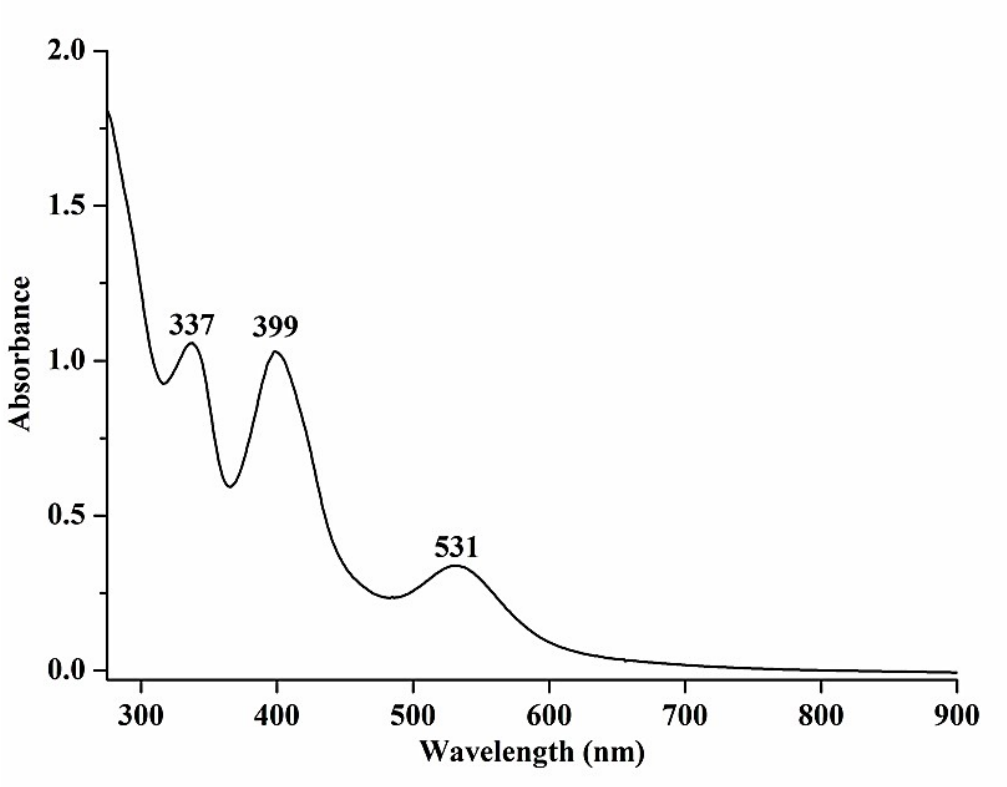

Figure S11. UV-visible spectrum of complex **1a** in CH_2Cl_2 at room temperature.

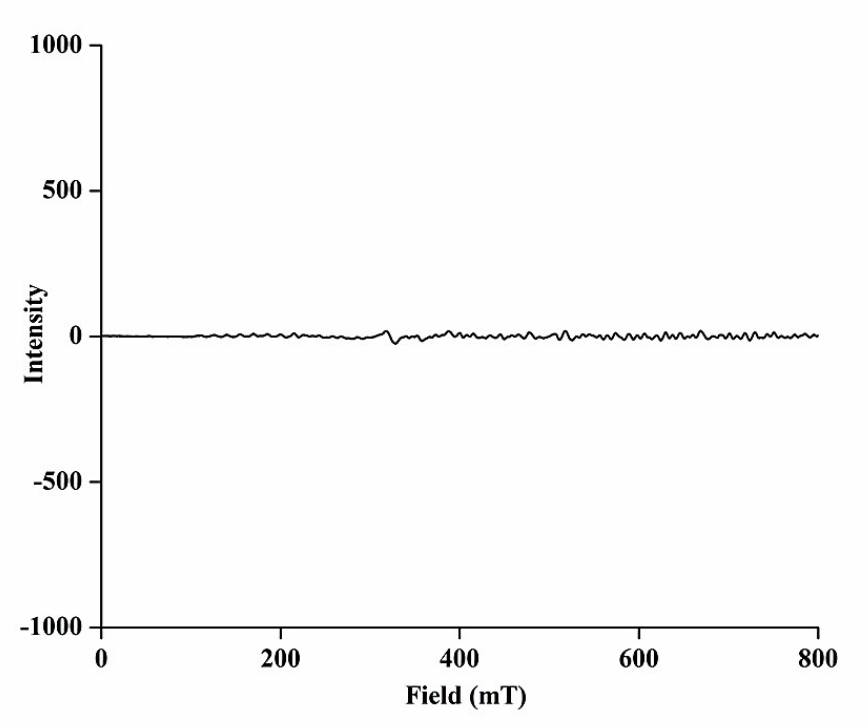

Figure S12. X-band EPR spectrum of complex **1a** in CH_2Cl_2 at 77 K.

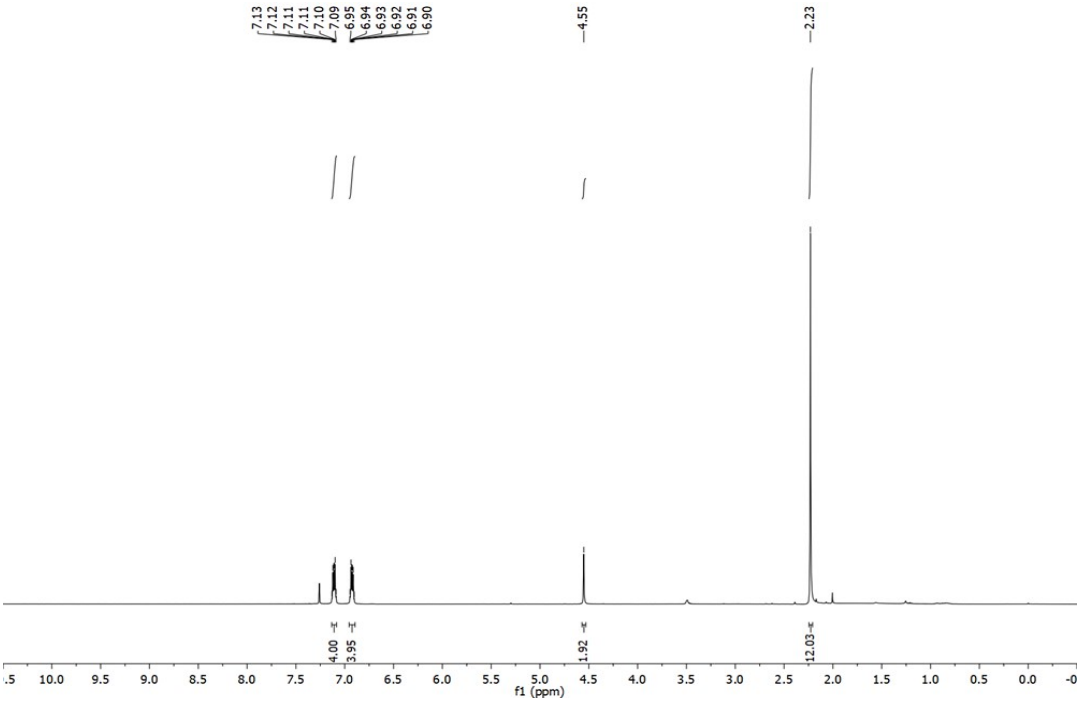

Figure S13. ^{1}H-NMR spectrum of complex **1a** in $CDCl_3$.

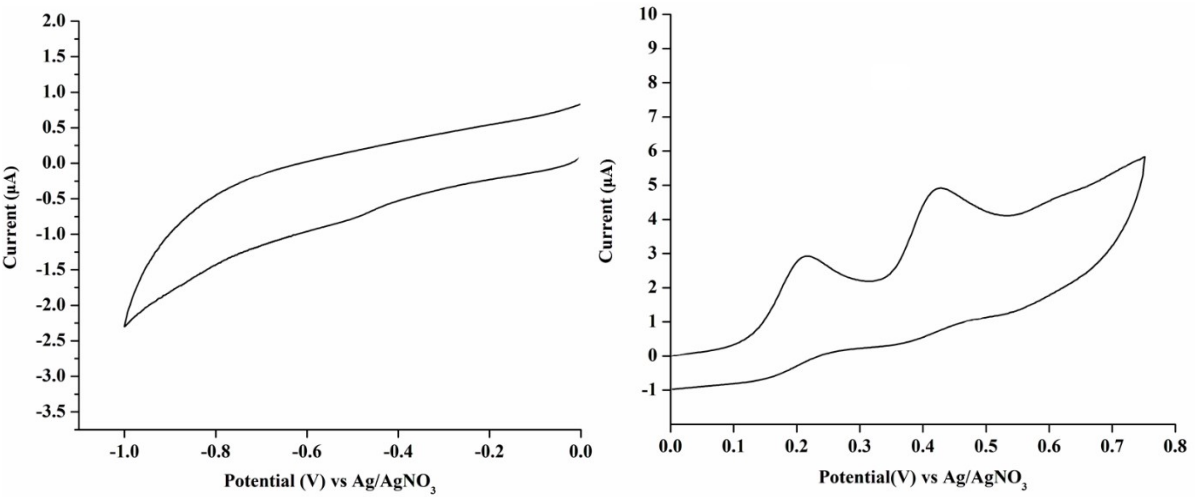

Figure S14. Cyclic voltammograms of complex **1a** in CH_2Cl_2 vs. $Ag/AgNO_3$, supporting electrolyte 0.1 M, Scan rate 0.1 v/s, at room temperature.

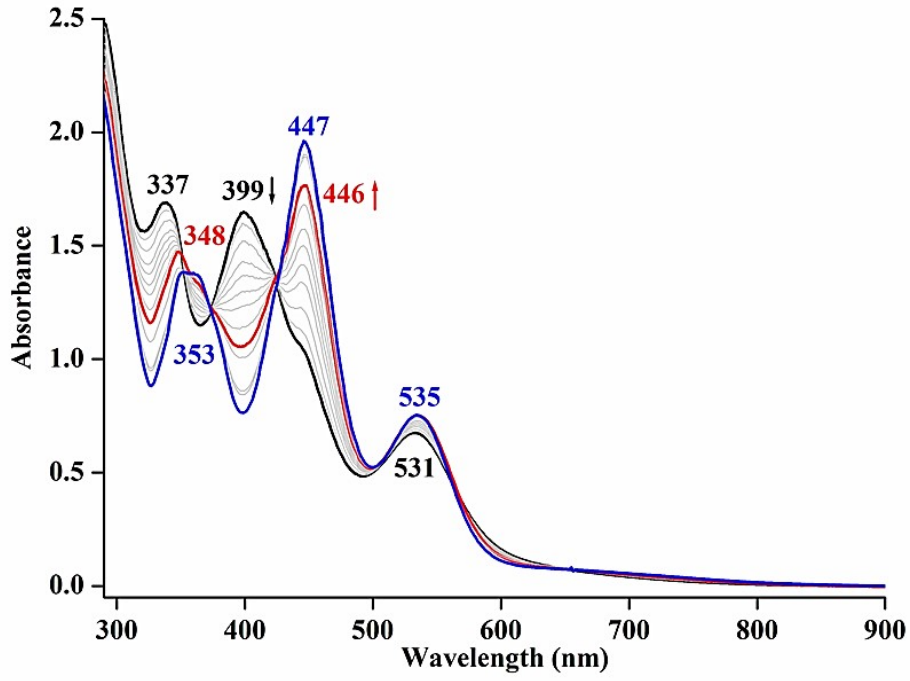

Figure S15. UV-visible spectral monitoring of complex **1a** (black), followed by addition of imidazole (red) then $NaBPh_4$ (blue) in CH_2Cl_2 at room temperature.

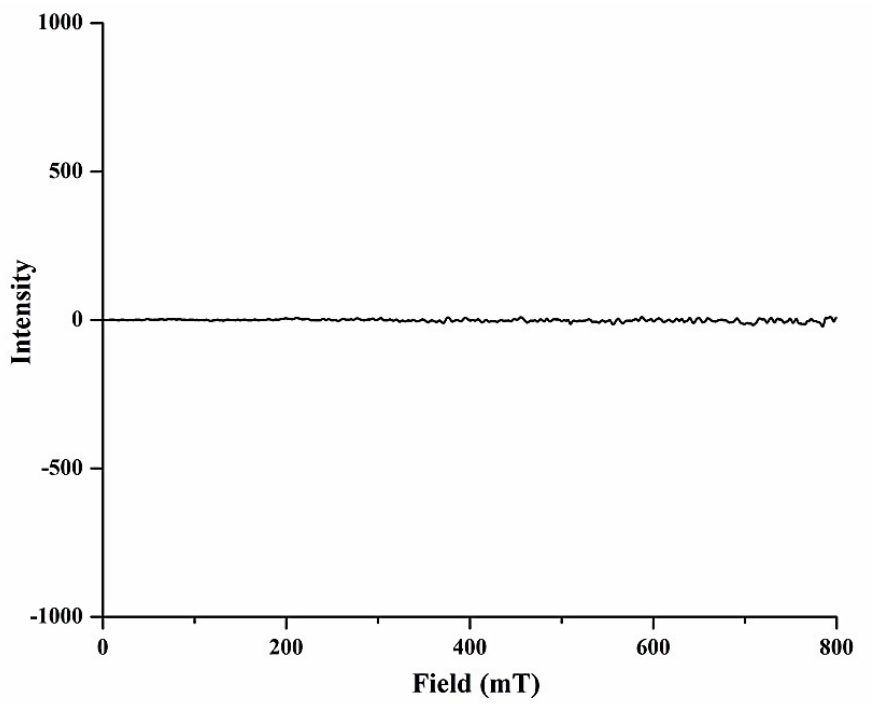

Figure S16. X-band EPR-spectrum of $[Co^{III}(TMTAA^{2-})(IM)]^{+}$ in CH_2Cl_2 at 77 K.

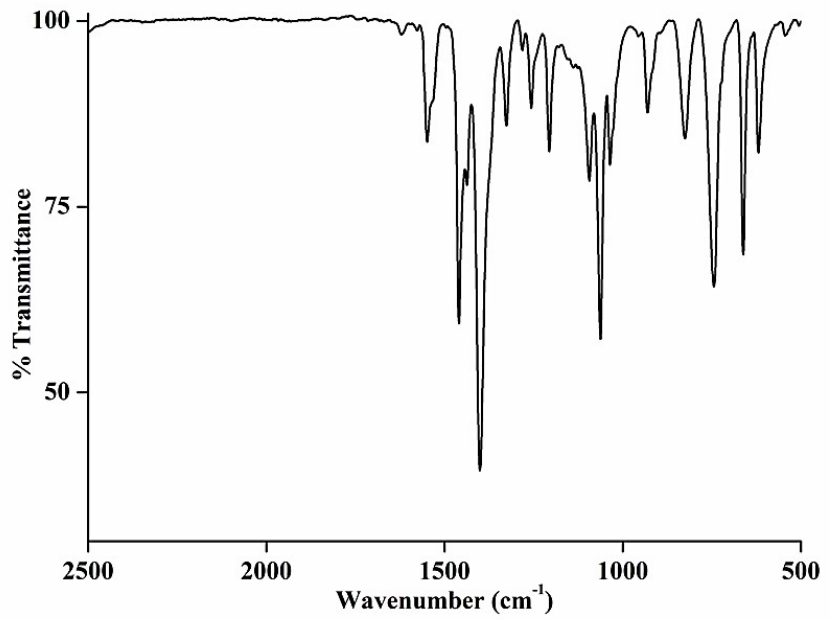

Figure S17. FT-IR spectrum of complex **2** in ATR probe.

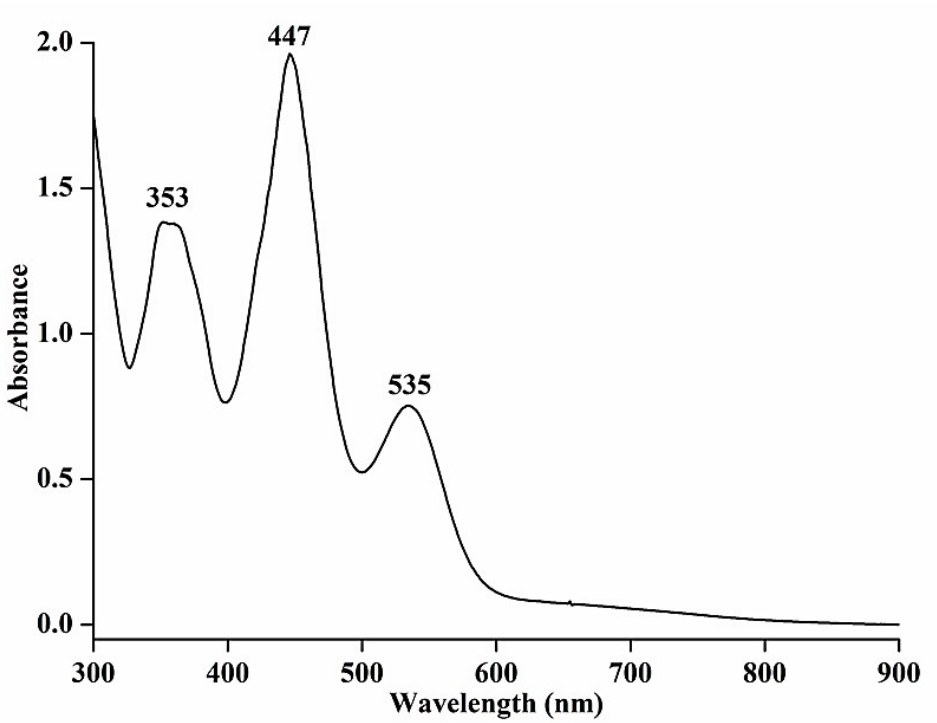

Figure S18. UV-visible spectrum of complex **2** in CH_2Cl_2 at room temperature.

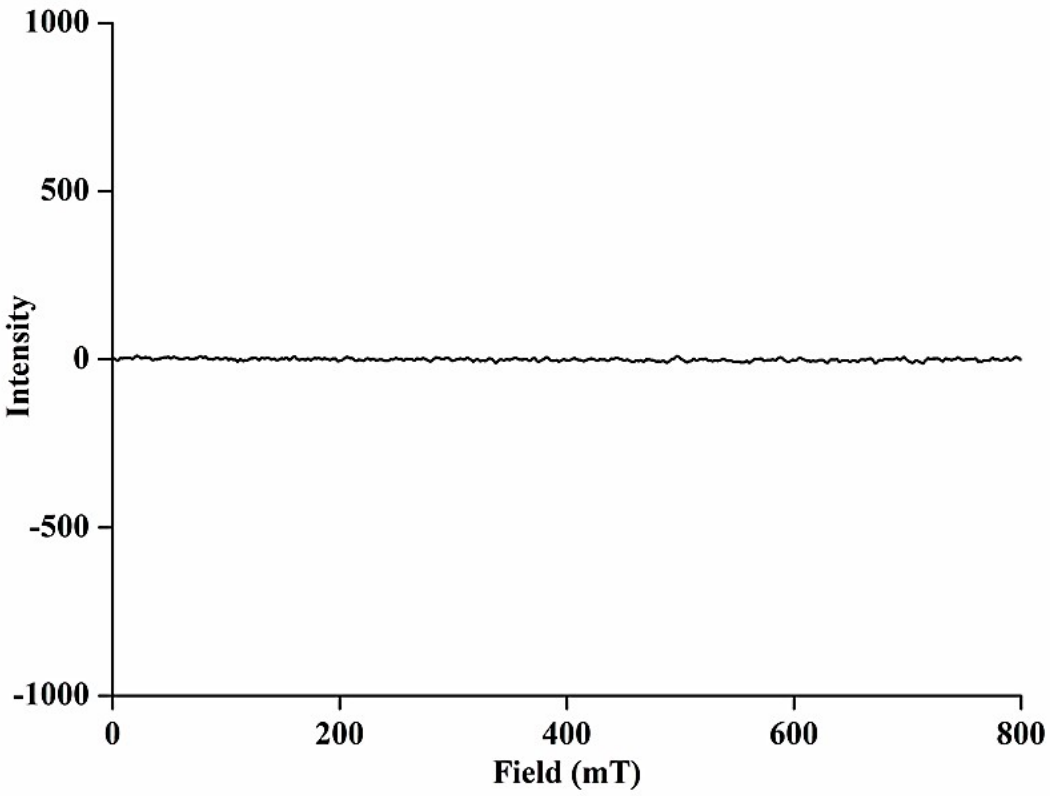

Figure S19. X-band EPR spectrum of complex **2** in CH_2Cl_2 at 77 K.

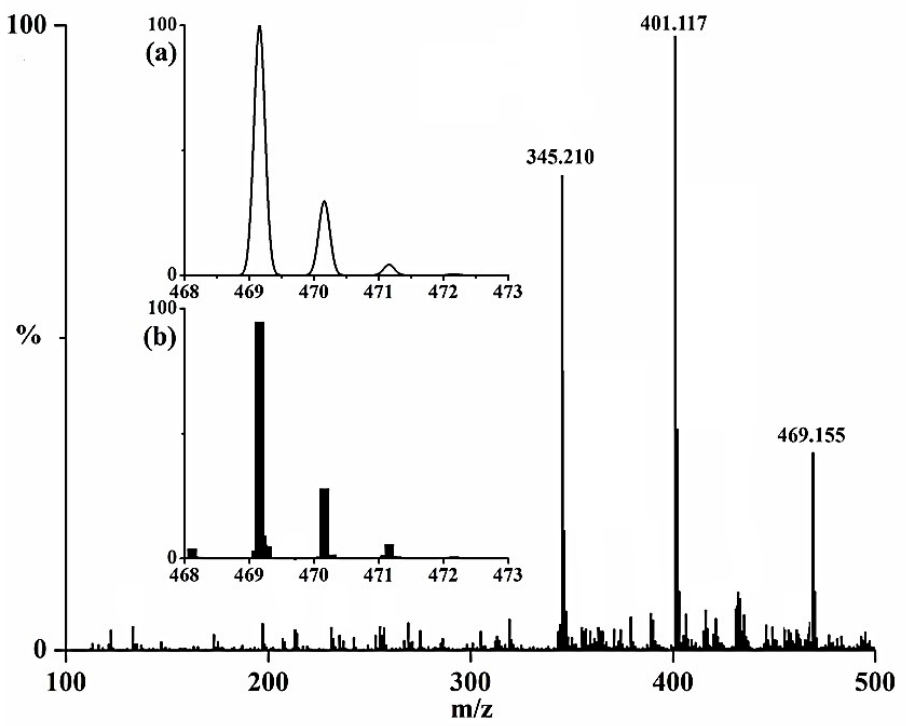

Figure S20. ESI-mass spectrum of Complex **2** in CH_3CN **(**Calculated, 469.155; Found, 469.155; After loss of BPh_4 unit. Inset: Isotopic distribution pattern; (a) Simulated, (b) Experimental).

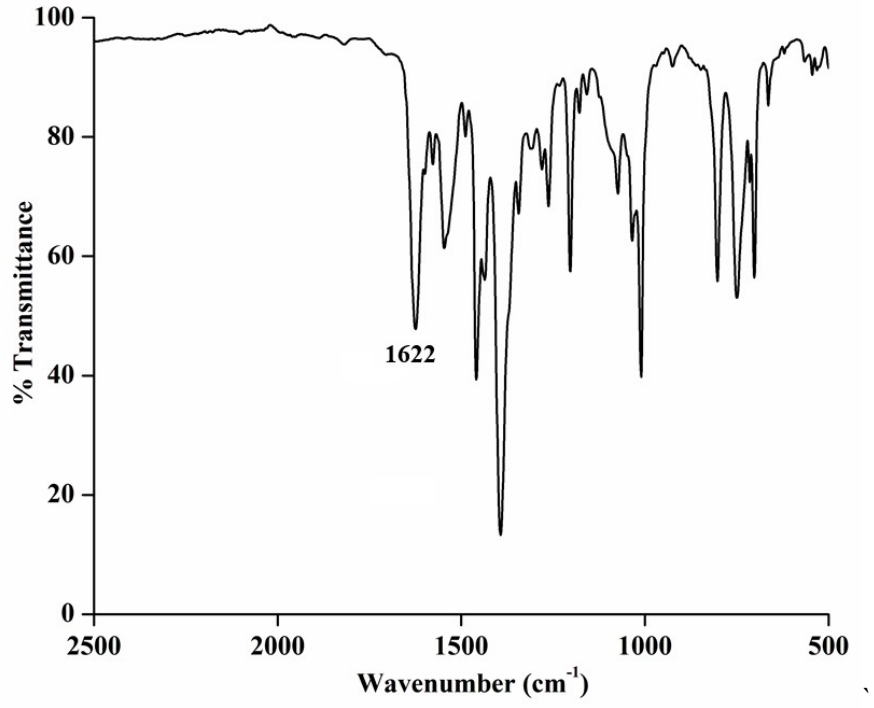

Figure S21. FT-IR spectrum of the reaction mixture of complex **1a** and $[Mn^{III}(TPP^{2-})Cl]$ in ATR probe.

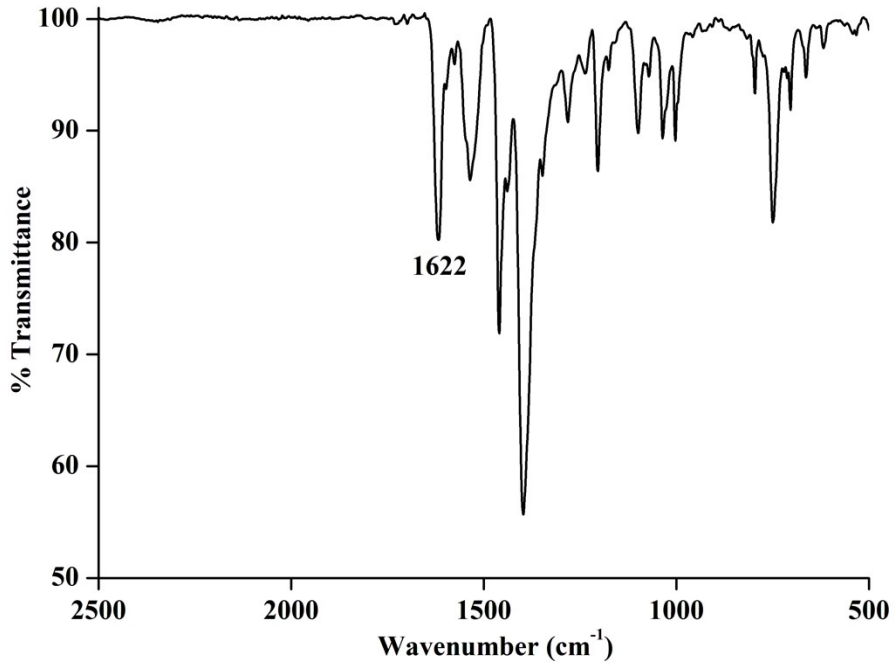

Figure S22. FT-IR spectrum of the reaction mixture of complex **1a** and [$Fe^{III}(TPP^{2-})Cl$] in ATR probe.

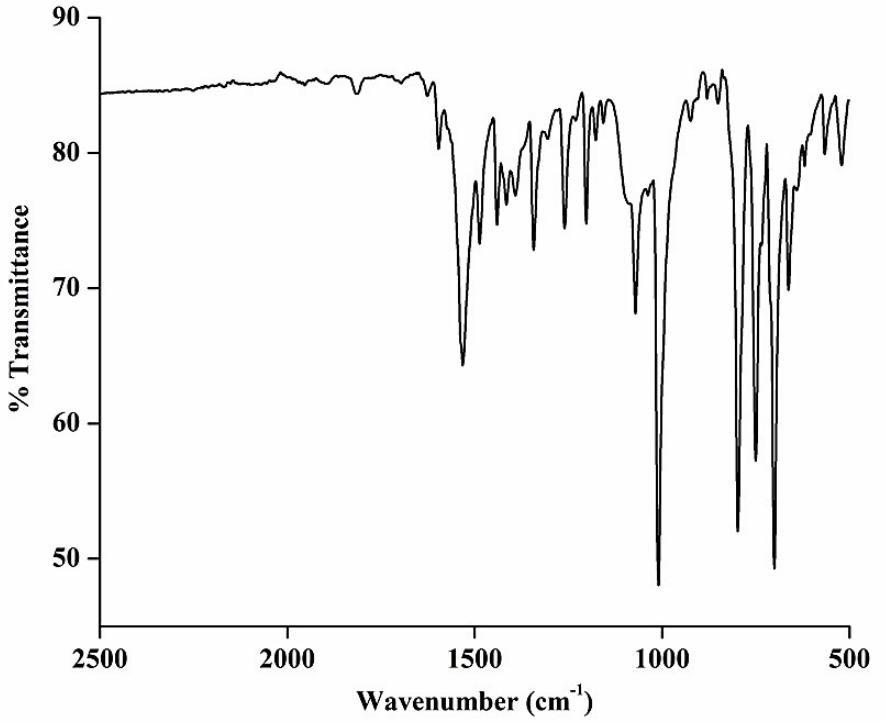

Figure S23. FT-IR spectrum of complex [$Mn^{III}(TPP^{2-})Cl$] in ATR probe.

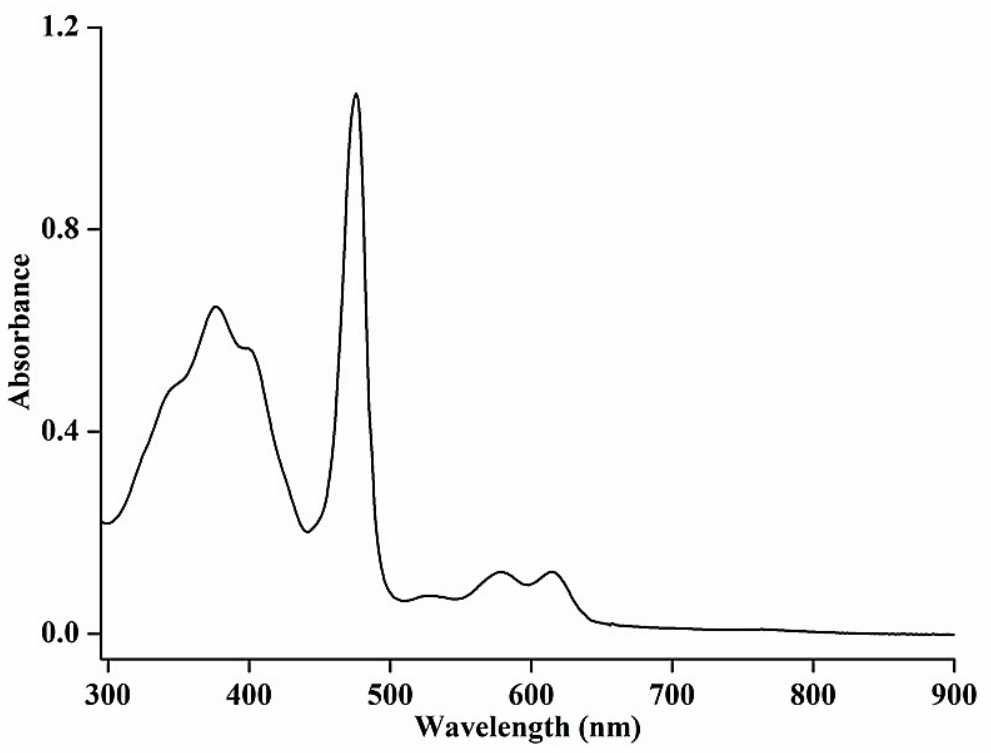

Figure S24. UV-visible spectrum of $[Mn^{III}(TPP^{2-})Cl]$ in CH_2Cl_2 at room temperature.

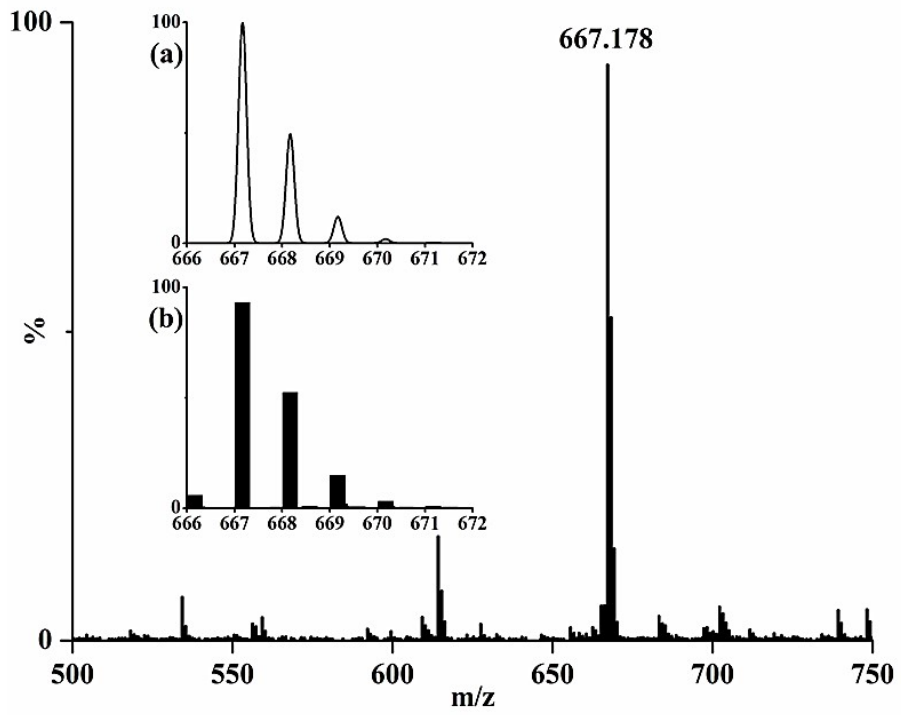

Figure S25. ESI-mass spectrum of $[Mn^{III}(TPP^{2-})Cl]$ in CH_3CN **(**Calculated, 667.169; Found, 667.178; after loss of Cl^-. Inset: Isotopic distribution pattern; (a) Simulated, (b) Experimental).

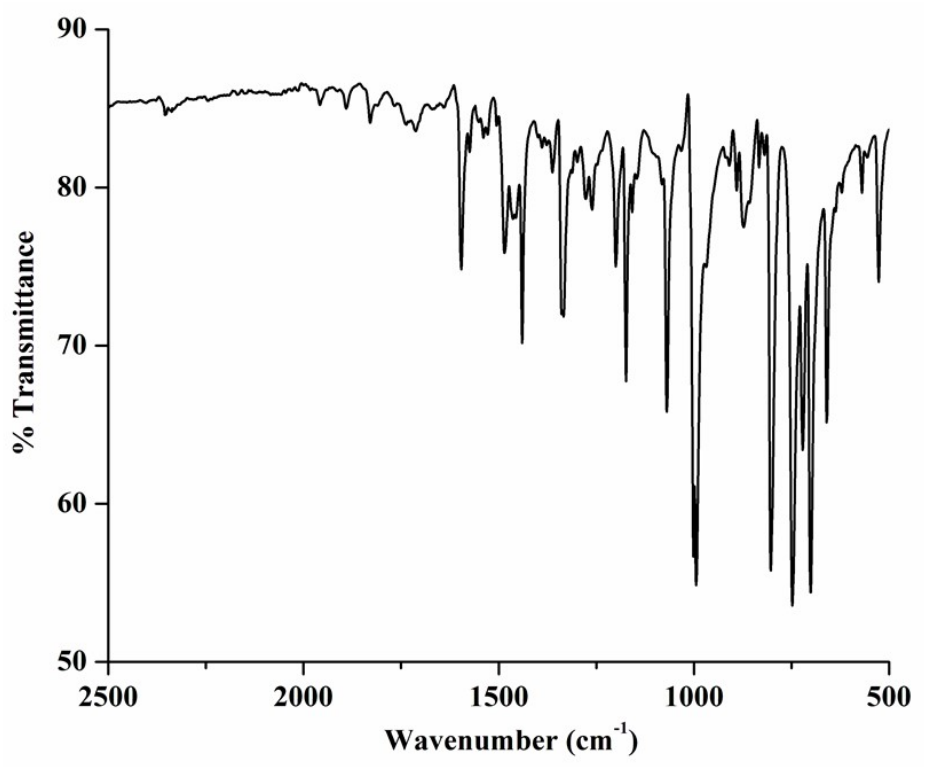

Figure S26. FT-IR spectrum of complex [$Fe^{III}(TPP^{2-})Cl$] in ATR probe.

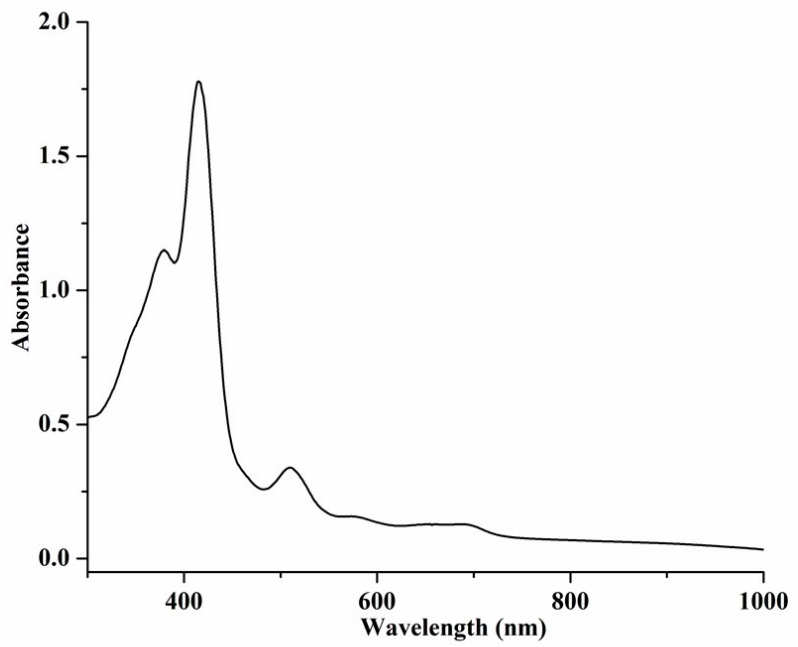

Figure S27. UV-visible spectrum of [$Fe^{III}(TPP^{2-})Cl$] in CH_2Cl_2 at room temperature.

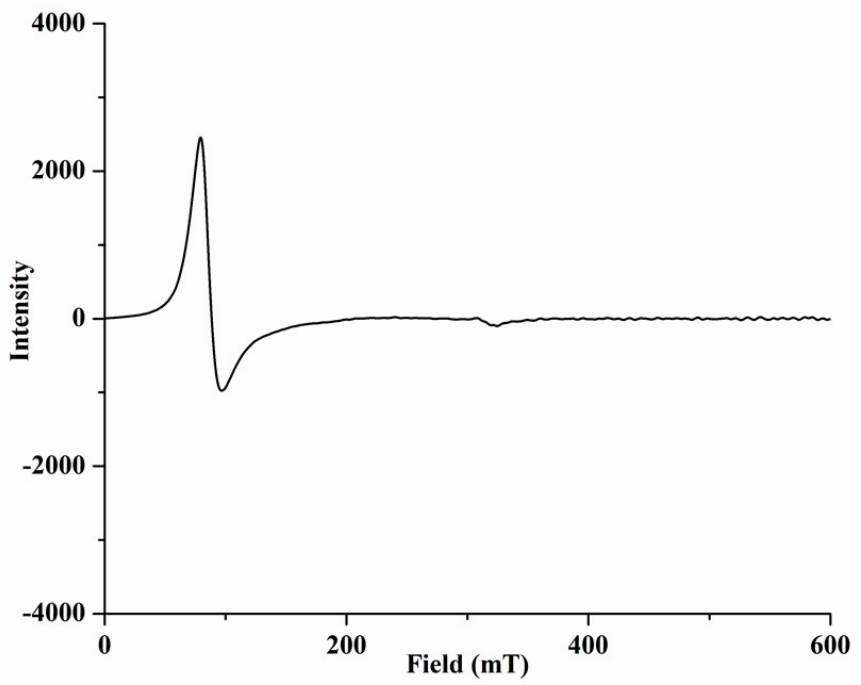

Figure S28. X-band EPR spectrum of [$Fe^{III}(TPP^{2-})Cl$] in CH_2Cl_2 at 77 K.

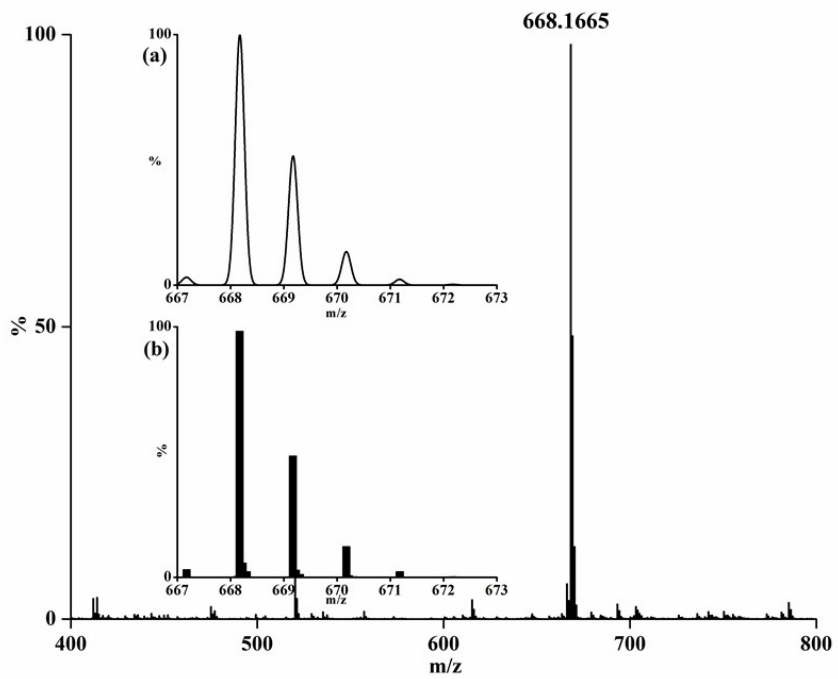

Figure S29. ESI-mass spectrum of [$Fe^{III}(TPP^{2-})Cl$] in CH_3CN **(**Calculated, 668.166; Found, 668.166; after loss of Cl^-. Inset: Isotopic distribution pattern; (a) Simulated, (b) Experimental).

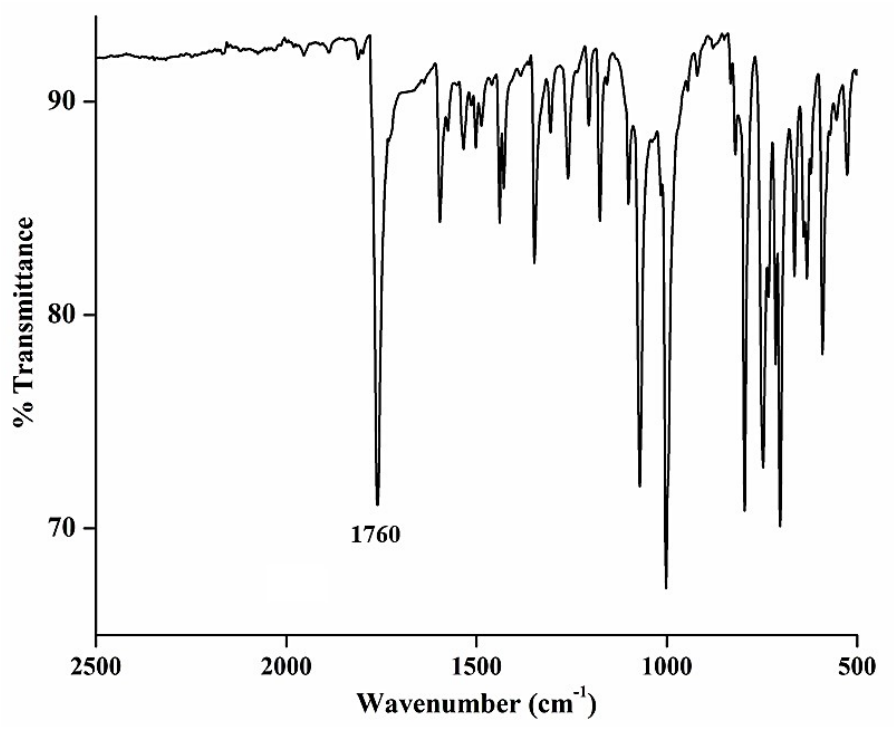

Figure S30. FT-IR spectrum of complex [Mn(TPP^{2-})(NO)] in ATR probe.

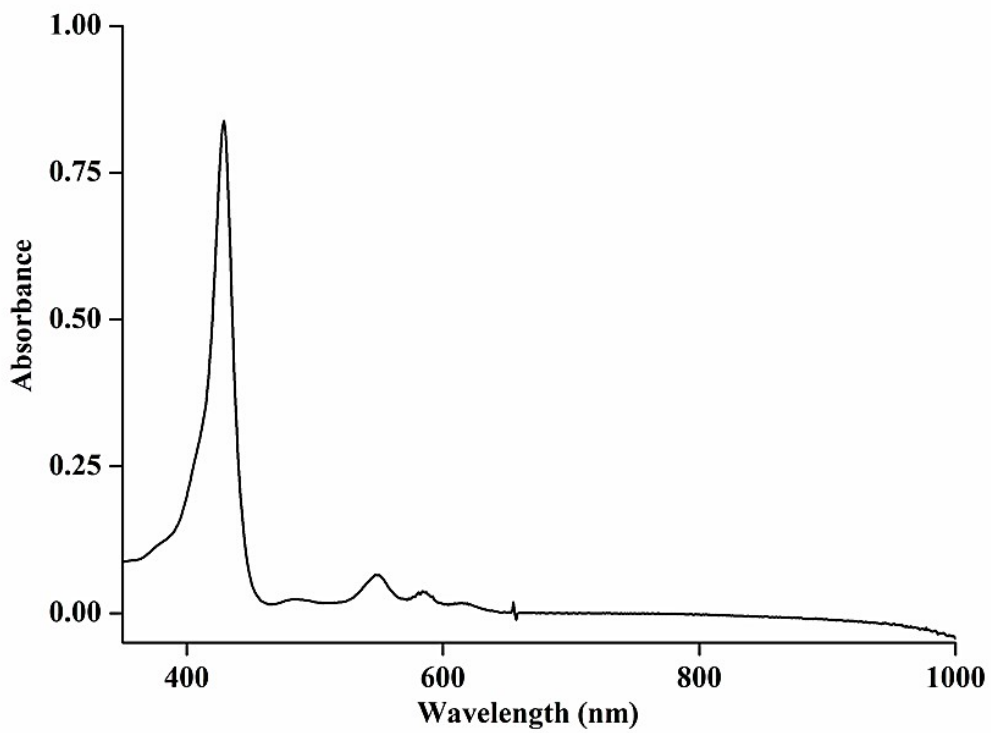

Figure S31. UV-visible spectrum of [Mn(TPP^{2-})(NO)] in CH_2Cl_2 at room temperature.

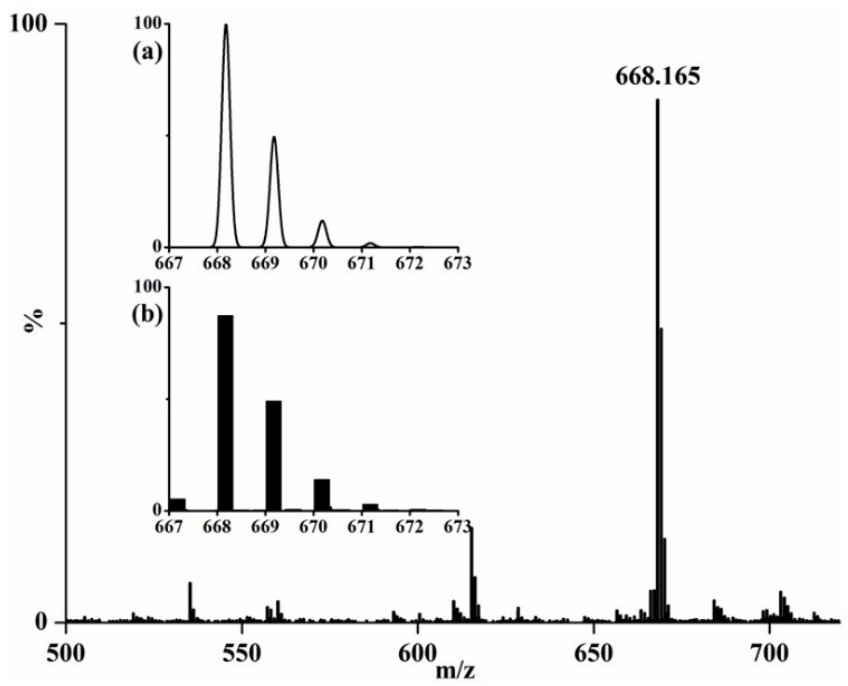

Figure S32. ESI-MS spectrum of [Mn(TPP^{2-})(NO)] in CH_3CN **(**Calculated, 668.177; Found, 668.165; After loss of NO, protonated. Inset: Isotopic distribution pattern; (a) Simulated, (b) Experimental).

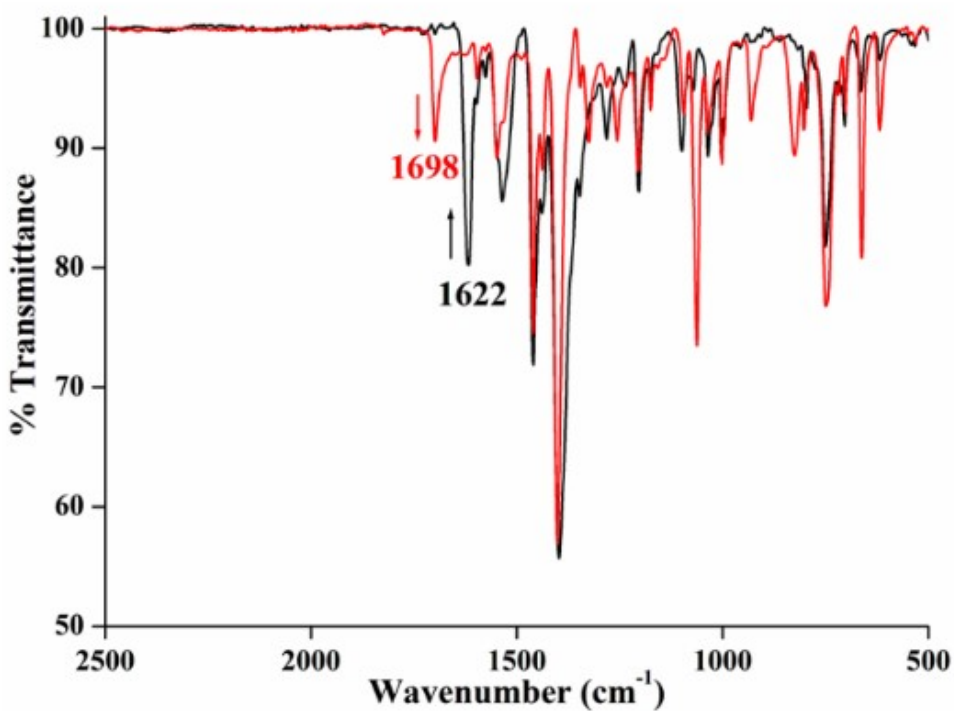

Figure S33. FT-IR (ATR probe) spectra of the reaction mixture of complex **1a** with [Fe^{III}(TPP^{2-})Cl] in the absence (black) and presence (red) of imidazole.

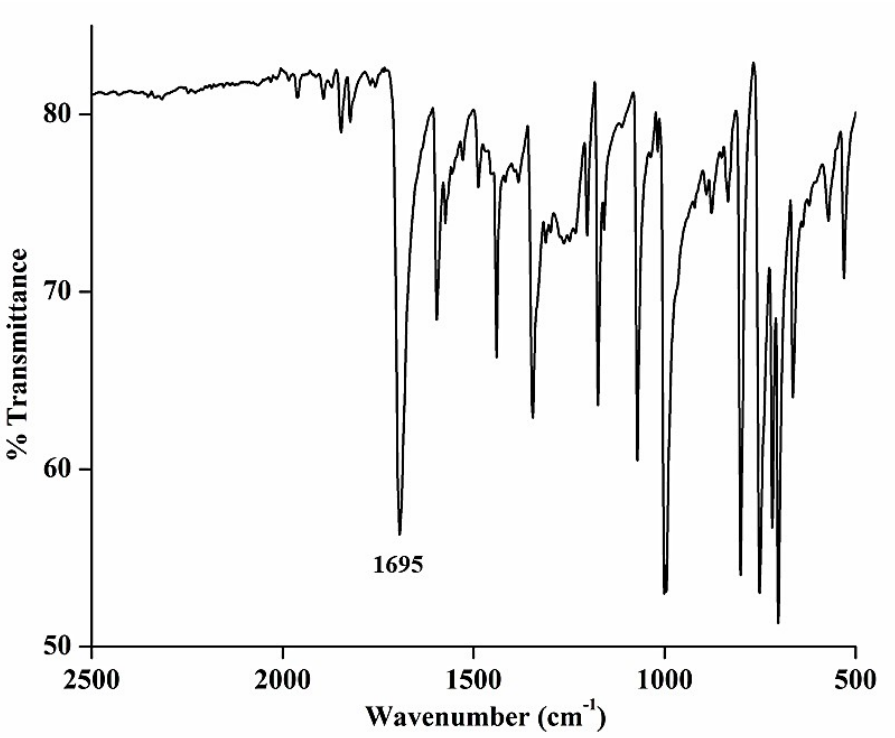

Figure S34. FT-IR spectrum of complex [Fe(TPP^{2-})(NO)] in ATR probe.

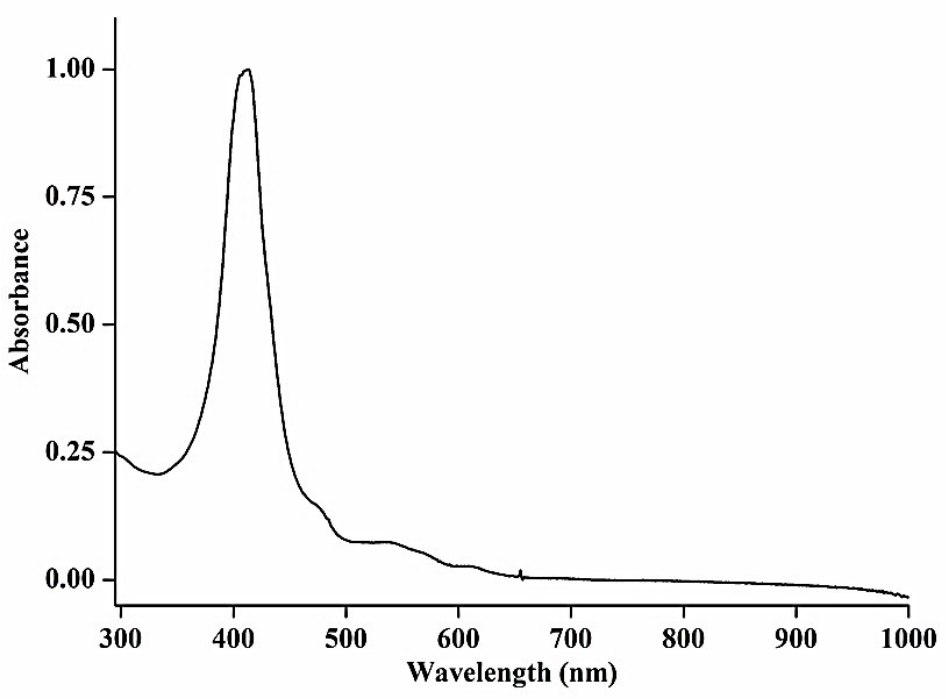

Figure S35. UV-visible spectrum of [Fe(TPP^{2-})(NO)] in CH_2Cl_2 at room temperature.

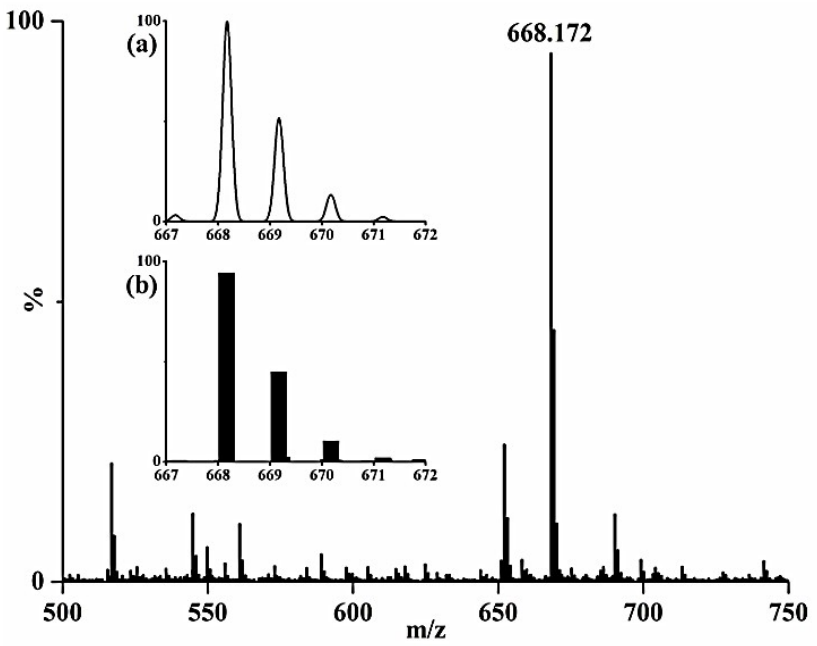

Figure S36. ESI-mass spectrum of [Fe(TPP^{2-})(NO)] in CH_3CN **(**Calculated, 668.166; Found, 668.172; After loss of NO, Inset: Isotopic distribution pattern; (a) Simulated, (b) Experimental)

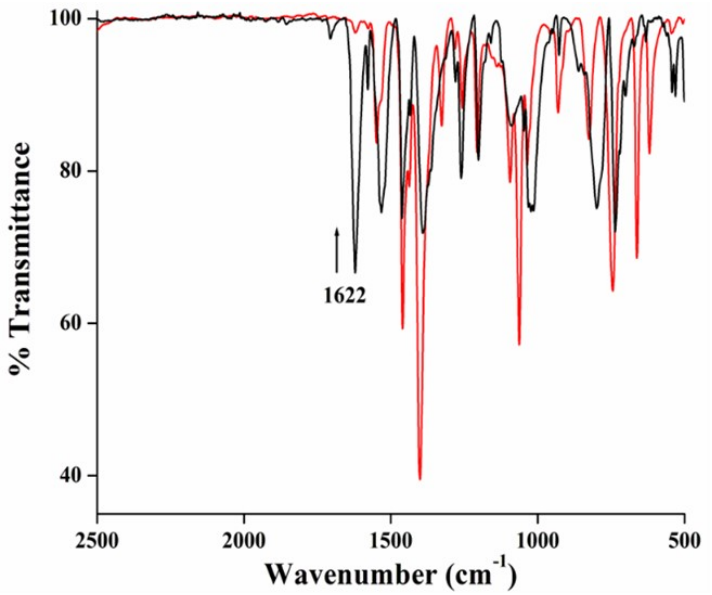

Figure S37. FT-IR (ATR probe) spectral monitoring of complex **1a** in the absence (black) and presence (red) of imidazole in CH_2Cl_2.

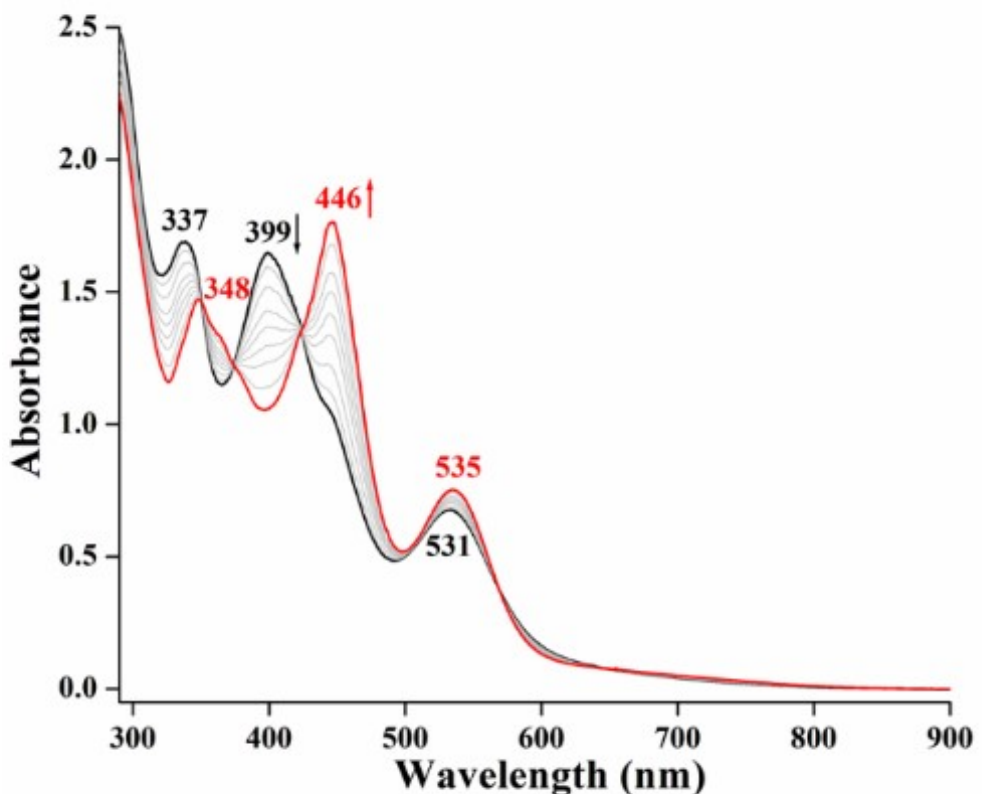

Figure S38. UV-visible (room temperature) spectral monitoring of complex **1a** in the absence (black) and presence (red) of imidazole in CH_2Cl_2.

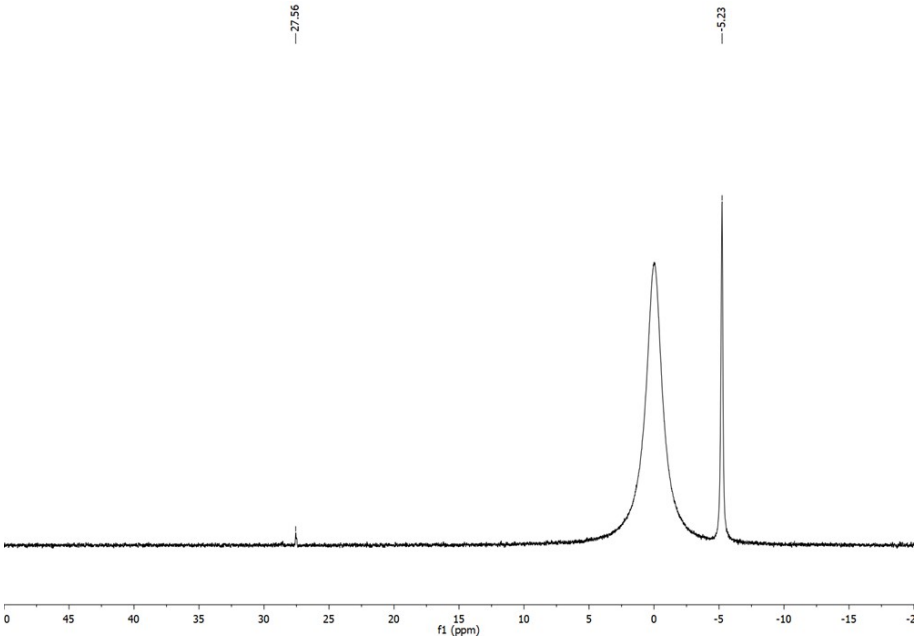

Figure S39. ^{31}P-NMR of the reaction mixture of complex **1a**, PPh_3 and imidazole in CH_2Cl_2 solution with 0.1 mL DMSO-d_6.

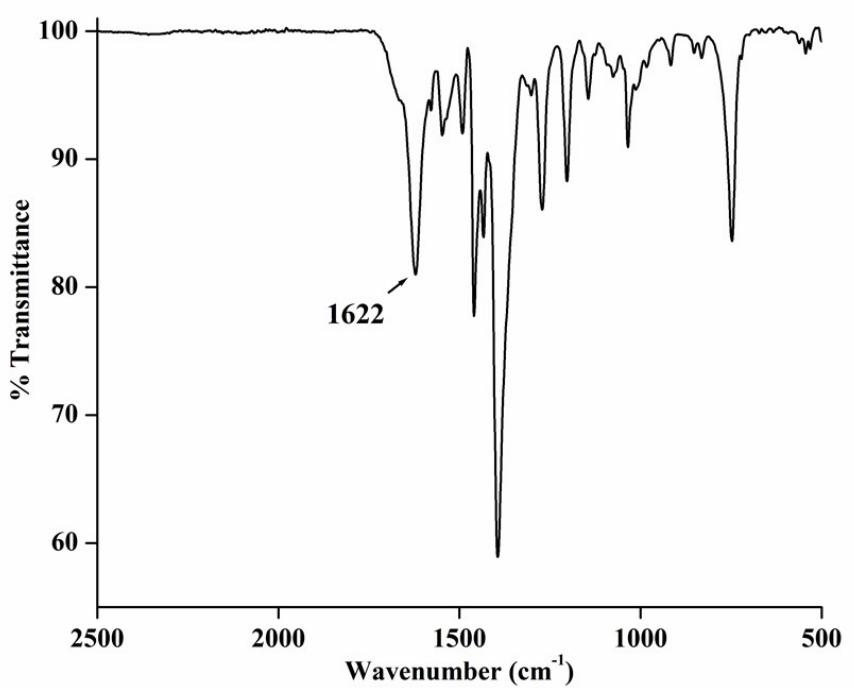

Figure S40. FT-IR spectrum of the reaction mixture of complex **1a** and PMe_3 after 24 hours in ATR probe.

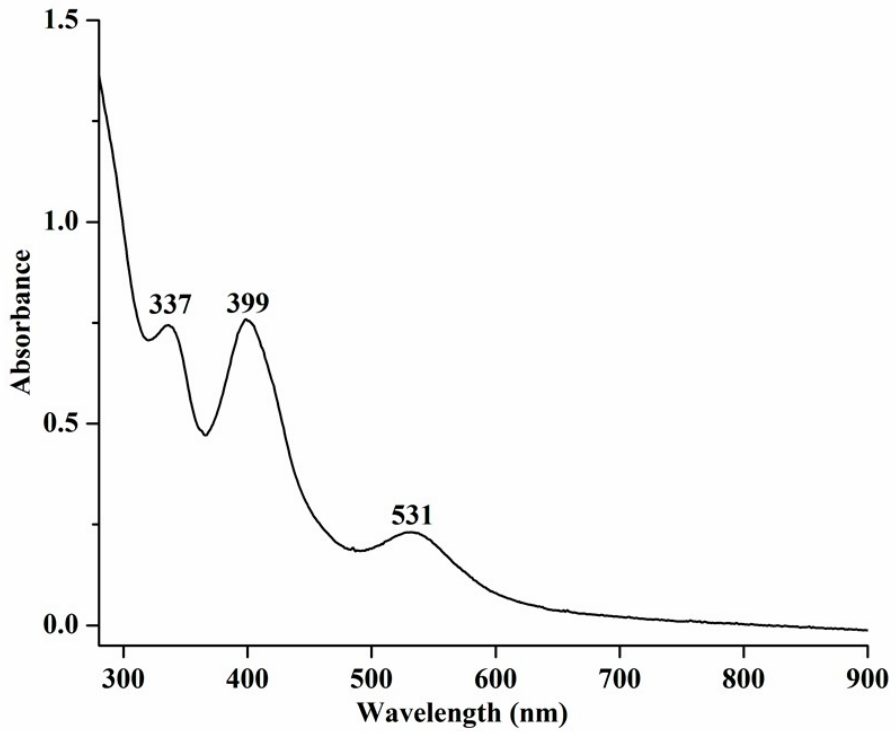

Figure S41. UV-visible spectrum of the reaction mixture of complex **1a** and PMe_3 in CH_2Cl_2 after 24 hours.

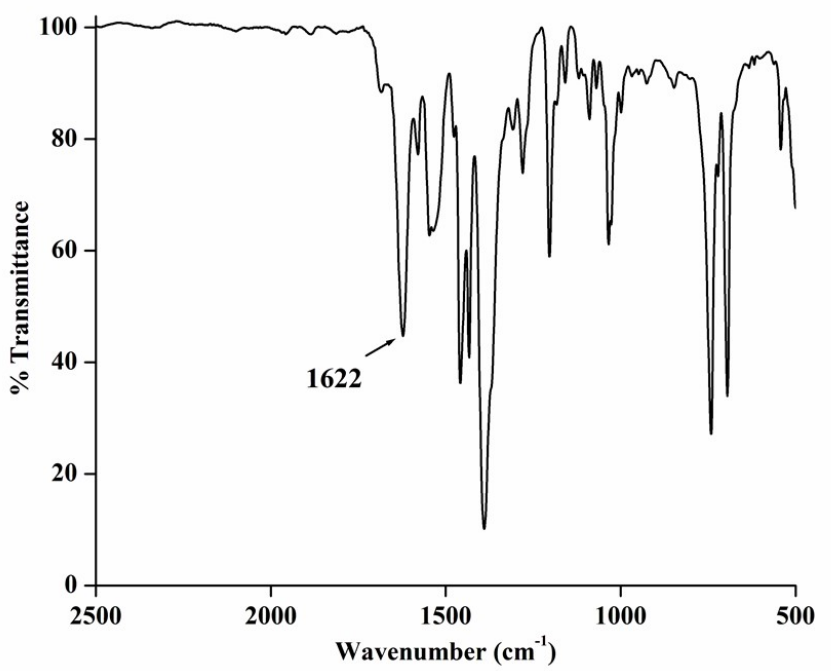

Figure S42. FT-IR spectrum of the reaction mixture of complex **1a** and PPh_3 after 24 hours in ATR probe.

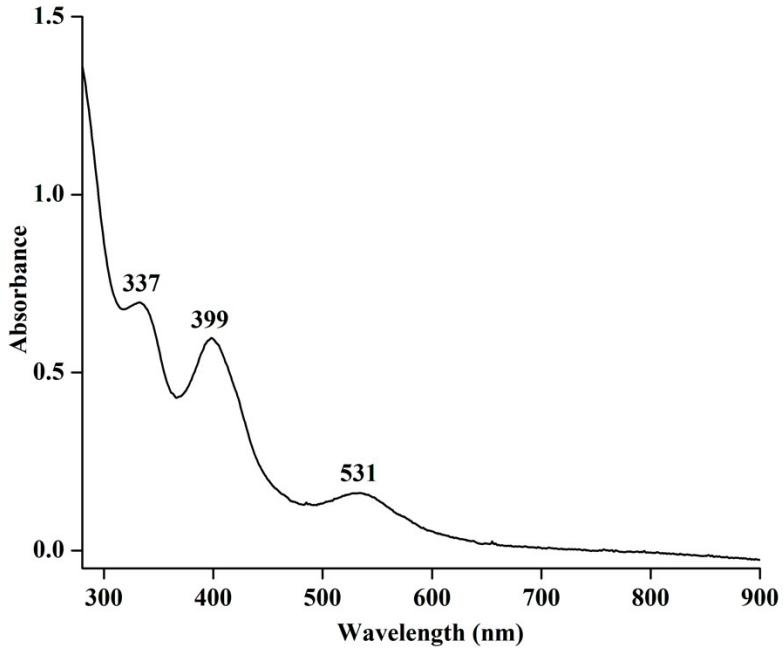

Figure S43. UV-visible spectrum of the reaction mixture of complex **1a** and PPh_3 in CH_2Cl_2 after 24 hours.

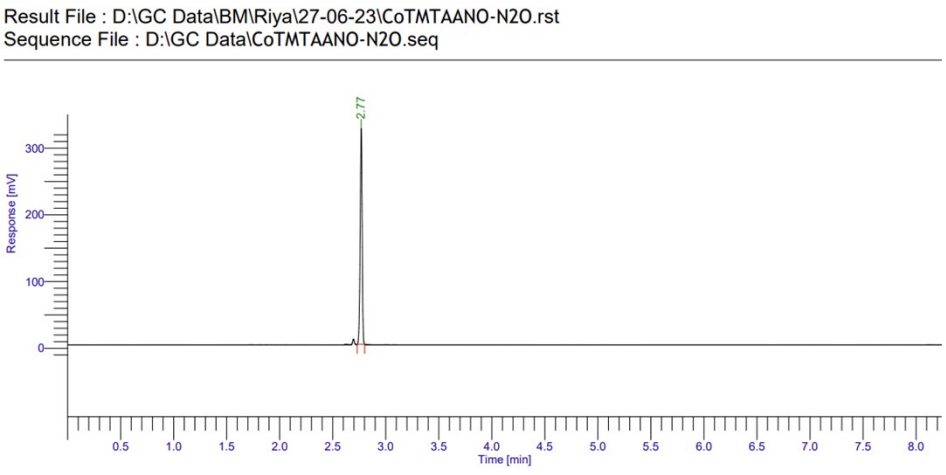

IIT Guwahati Chemistry Dept.

Peak #	Component Name	Time [min]	Area [uV*sec]	Height [uV]	Area [%]
1		2.768	417386.88	323732.56	100.00
			417386.88	323732.56	100.00

Figure S44. Gas chromatograms of headspace gas of the reaction mixture of complex **1a** and imidazole in presence of HBF_4 (retention time = 2.77 min).

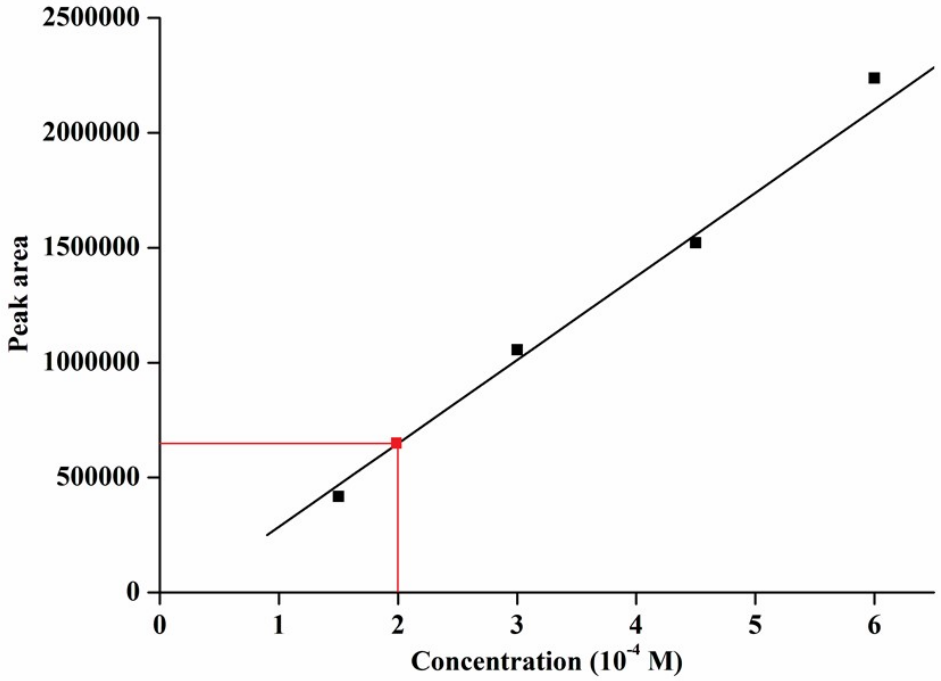

Figure S45. GC calibration curve for determination of amount of N_2O (red line corresponds to the sample).

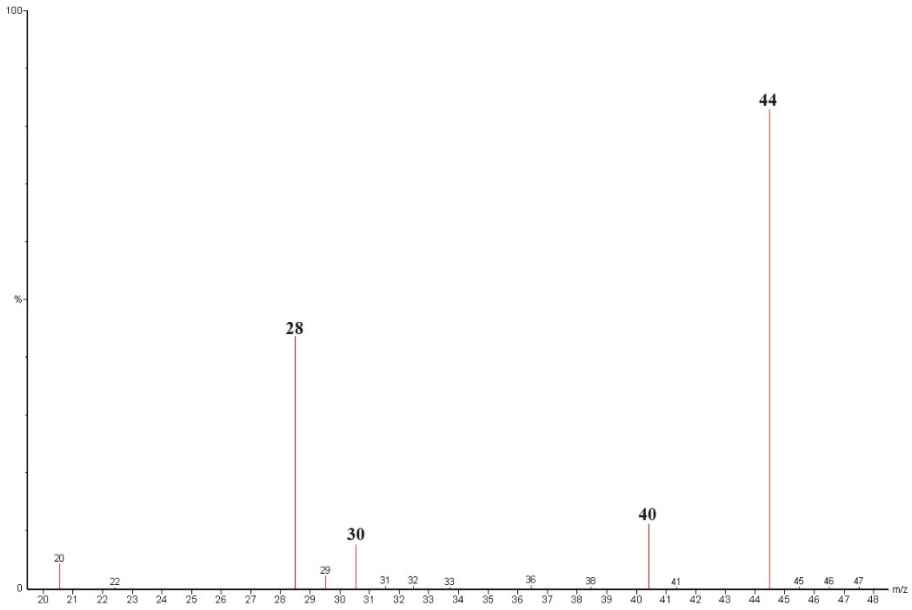

Figure S46. GC-mass spectrum of the headspace gas of the reaction mixture of complex **1a** and imidazole in presence of HBF_4.

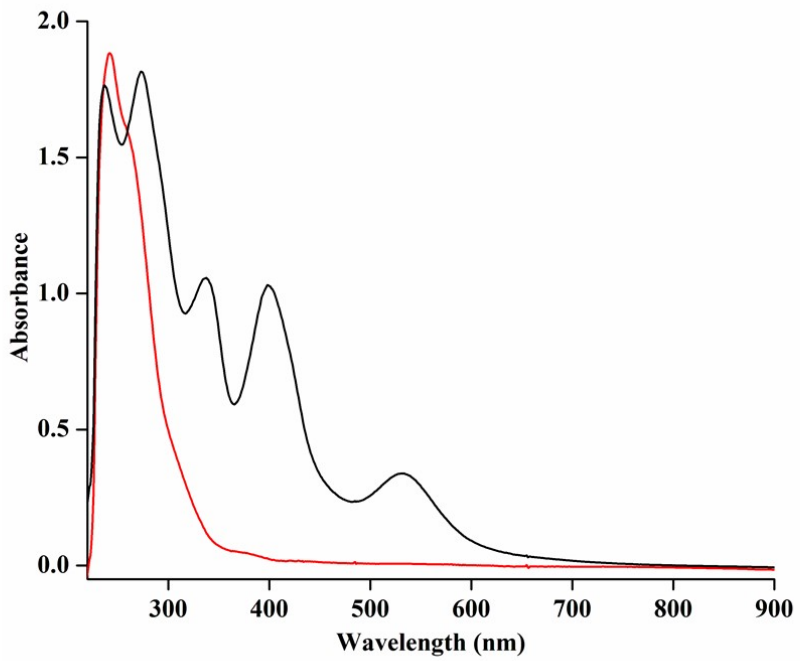

Figure S47. UV-visible spectra of complex **1a** before (black) and after (red) addition of $HBF_4.Et_2O$ in CH_2Cl_2 at room temperature.

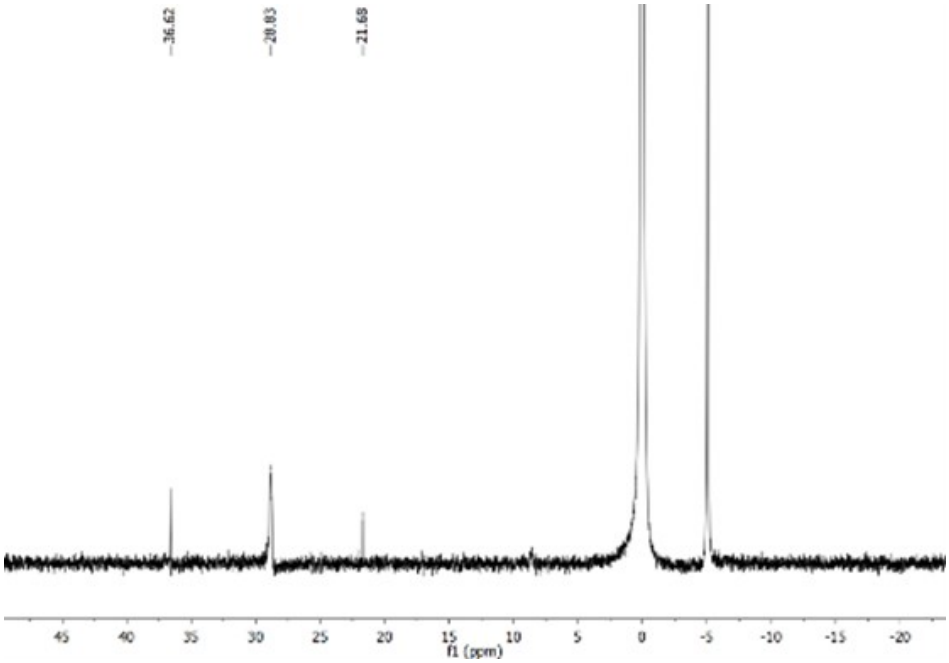

Figure S48. ^{31}P-NMR of the reaction mixture of complex **1a**, imidazole, PPh_3 and HBF_4 in CH_2Cl_2 solution with 0.1 mL DMSO-d_6.

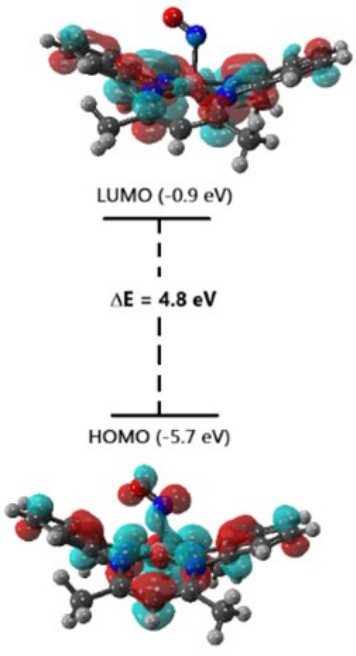

Figure S49. Shapes and energies (eV) of HOMO and LUMO of complex **1a**.

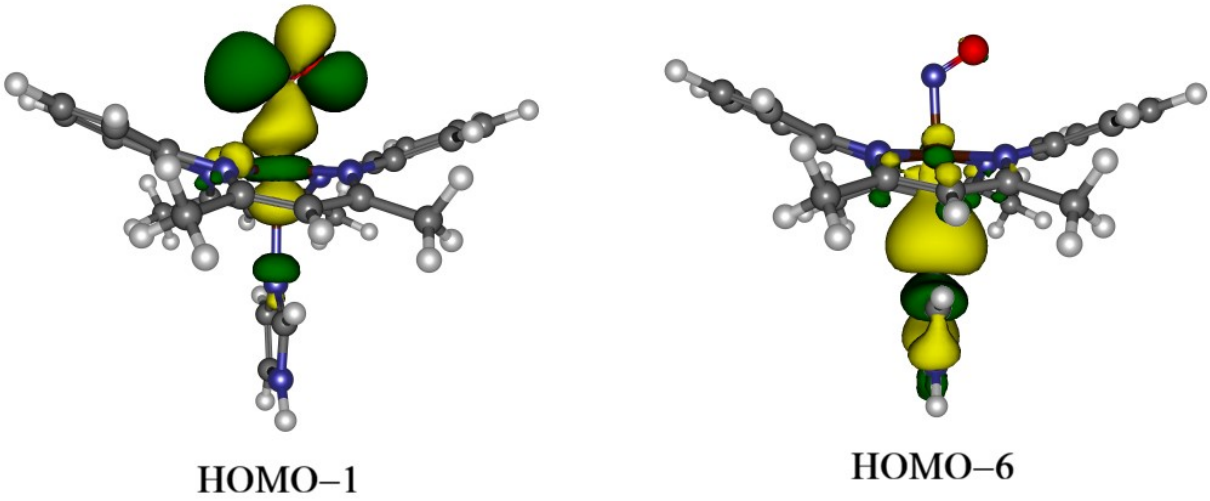

Figure S50. Key occupied frontier orbitals representing Co-NO interaction (HOMO-1) and Co-imidazole interaction (HOMO-6).

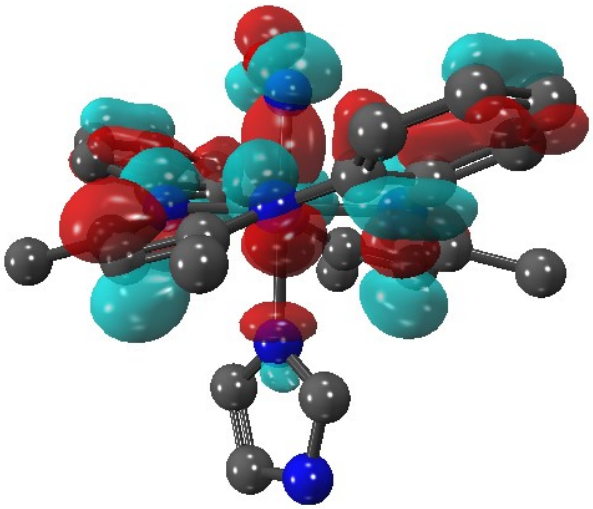

Figure S51. Highest occupied molecular orbital (HOMO) of the intermediate **1b**.

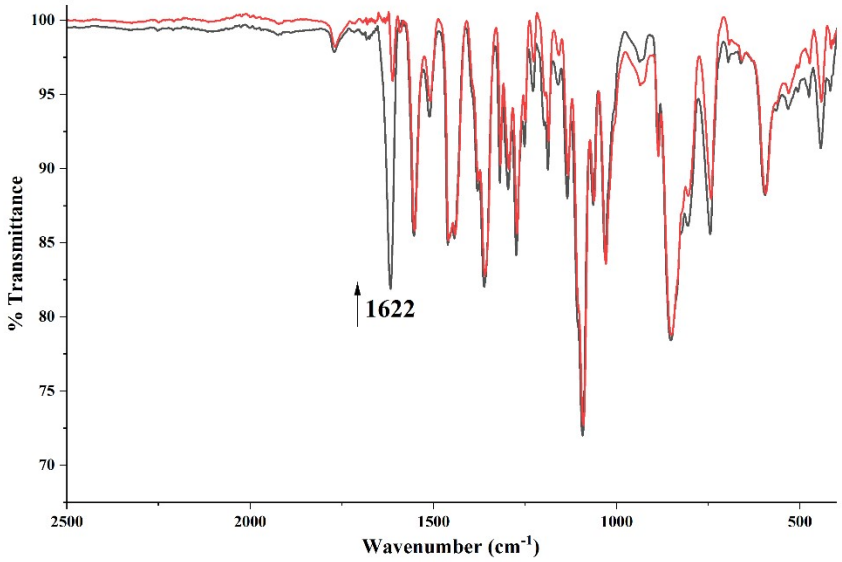

Figure S52. FT-IR spectra illustrating the reaction of complex **1a** with morpholine in dry dichloromethane at room temperature. The black trace represents the spectrum recorded immediately after mixing, while the red trace corresponds to the spectrum obtained after 1 h. A gradual decrease in the ν(NO) band at 1622 cm^{-1} is observed.

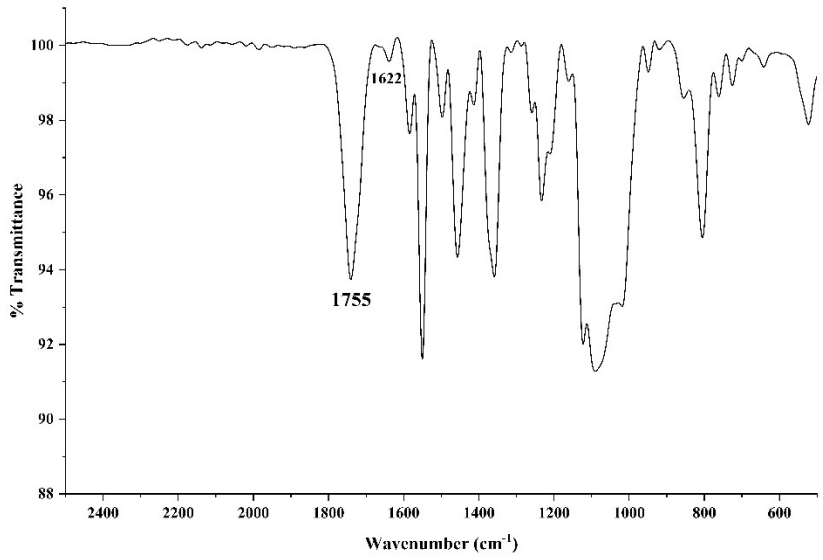

Figure S53. FT-IR spectrum of the reaction mixture obtained from complex **1a**, [Mn^{III}(TPP)Cl], and morpholine in dry dichloromethane after 1 h. The ν(NO) band of complex 1a at 1622 cm^{-1} disappears, while a new band at 1755 cm^{-1} corresponding to [Mn(TPP)(NO)] is observed.

Table S1. List of cobalt-nitrosyl complexes and their respective NO stretching frequencies.

Complex	ν_{NO} (cm^{-1})	Co-N_{NO} (Å)	N-O (Å)	Co-N_{NO}-O (°)	Ref.
$[(14\text{-TMC})Co^{III}(NO)]^{2+}$	1715	1.901	1.152	129.35	7a
$[(13\text{-TMC})Co^{III}(NO)]^{2+}$	1716	1.797(4)	1.159(5)	124.4(3)	7b
$[(12\text{-TMC})Co^{III}(NO)]^{2+}$	1712	1.7844(14)	1.155(2)	128.50(13)	7b
[(BPI)Co(NO)(OAc)]	1673	1.828(8)	1.014(8)	132.7(7)	7c
$[Co(LN_4^{PhCl})(NO)]$	1667	1.798(3)	1.172(4)	124.4(3)	8
[Co(BPB)(NO)]	1662	1.791(6)	1.119(10)	130.2(7)	9
$[Co(L_2)(NO)Cl]Cl$	1659	1.765	1.103(9)	124.57(5)	7d
$[Co(TMTAA^{2-})(NO)]$ (**1a**)	1622	1.818(3)	1.124(5)	125.1(3)	This work

Table S2. Crystallographic data for complexes **1** and **1a**.

	1	**1a**
Formulae	$C_{44}H_{44}Co_2N_8$	$C_{23}Cl_2CoN_5OH_{24}$
Mol. wt.	802.73	516.30
Crystal system	Monoclinic	Triclinic
Space group	$P2_1/c$	P-1
Temperature /K	293(2)	296.0
Wavelength /Å	0.71073	0.71073
a /Å	14.4344(8)	9.1802(8)
b /Å	16.4066(5)	11.2850(10)
c /Å	16.2778(7)	12.0488(10)
α/°	90	102.415(3)
β/°	99.840(4)	94.370(3)
γ/°	90	104.862(3)

V/ Å3	3798.2(3)	1166.81(18)
Z	4	2
Density/Mgm-**3**	1.404	1.470
Abs. Coeff. /mm-**1**	0.917	0.990
Abs. correction	none	none
F(000)	1672	532
Total no. of reflections	6684	4111
Reflections, $I > 2\sigma(I)$	5141	3802
Max. 2θ/°	27.9930	27.83
Ranges (h, k, l)	$-17 \le h \le 15$ $-19 \le k \le 11$ $-14 \le l \le 19$	$-10 \le h \le 10$ $-13 \le k \le 13$ $-14 \le l \le 14$
Complete to 2θ (%)	0.999	1.000
Refinement method	Full-matrix least-squares on *F***2**	Full-matrix least-squares on *F***2**
Goof (*F2*)	0.998	1.095
R indices [$I > 2\sigma(I)$]	0.0453	0.0702
R indices (all data)	0.0659	0.0728
Largest diff. peak/hole / e Å^{-3}	0.51/-0.74	0.81/-0.72

Table S3. Selected bond lengths (Å) of complexes **1** and **1a**.

Atoms	**1**	**1a**
Co1-N1	1.908(2)	1.910(3)
Co1-N2	1.900(3)	1.910(3)
Co1-N3	1.901(2)	1.902(3)
Co1-N4	1.902(3)	1.907(3)
Co1-N5	-	1.818(3)
N5-O1	-	1.124(5)
Co2-N5	1.889(2)	-
Co2-N6	1.895(2)	-

Co2-N7	1.885(2)	-
Co2-N8	1.891(3)	-

Table S4. Selected bond angles (˚) of complexes **1** and **1a**.

Atoms	**1**	**1a**
N1-Co1-N2	84.57(10)	83.37(13)
N2-Co1-N3	95.49(11)	94.59(13)
N3-Co1-N4	89.46(9)	83.17(13)
N4-Co1-N1	84.56(10)	94.66(13)
Co1-N5-O1	-	125.1(3)
N1-Co1-N5	-	95.98(14)
N2-Co1-N5	-	97.17(14)
N3-Co1-N5	-	98.43(14)
N4-Co1-N5	-	99.59(14)

Reference

1. SMART, SAINT and XPREP, *Siemens Analytical X-ray Instruments Inc.*, Madison, Wiscoin, USA, 1995.
2. (a) G. M. Sheldrick, *Acta Crystallogr., Sect. A: Found. Adv.*, 2015, **71**, 3.
   (b) G. M. Sheldrick, *Acta Crystallogr., Sect. C: Struct. Chem.*, 2015, **71**, 3.
   (c) L. J. Farrugia, *J. Appl. Crystallogr.*, 1997, **30**, 565.
3. Y. Zhao and D. G. Truhlar, *Theor. Chem. Acc.*, 2008, **120**, 215–241.
4. Gaussian 16, Revision B.01, Gaussian 16, Revision B.01, M. J. Frisch, G. W. Trucks, H. B. Schlegel, G. E. Scuseria, M. A. Robb, J. R. Cheeseman, G. Scalmani, V. Barone, G. A. Petersson, H. Nakatsuji, X. Li, M. Caricato, A. V. Marenich, J. Bloino, B. G. Janesko, R. Gomperts, B. Mennucci, H. P. Hratchian, J. V. Ortiz, A. F. Izmaylov, J. L. Sonnenberg, D. Williams-Young, F. Ding, F. Lipparini, F. Egidi, J. Goings, B. Peng, A. Petrone, T. Henderson, D. Ranasinghe, V. G. Zakrzewski, J. Gao, N. Rega, G.

Zheng, W. Liang, M. Hada, M. Ehara, K. Toyota, R. Fukuda, J. Hasegawa, M. Ishida, T. Nakajima, Y. Honda, O. Kitao, H. Nakai, T. Vreven, K. Throssell, J. A. Montgomery Jr., J. E. Peralta, F. Ogliaro, M. J. Bearpark, J. J. Heyd, E. N. Brothers, K. N. Kudin, V. N. Staroverov, T. A. Keith, R. Kobayashi, J. Normand, K. Raghavachari, A. P. Rendell, J. C. Burant, S. S. Iyengar, J. Tomasi, M. Cossi, J. M. Millam, M. Klene, C. Adamo, R. Cammi, J. W. Ochterski, R. L. Martin, K. Morokuma, O. Farkas, J. B. Foresman and D. J. Fox, Gaussian, Inc., Wallingford, CT, 2016.

5. J. H. Niewahner, K. A. Walters and A. Wagner, *J. Chem. Educ.*, 2007, **84**, 477–479.
6. (a) G. A. Mirafzal, H. M. Bossé and J. M. Sumner, *Tetrahedron Lett.*, 1999, **40**, 623–626.

   (b) A. D. Adler, L. R. Longo, F. Kampas and J. Kim, *J. Inorg. Nucl. Chem.*, 1970, **32**, 2443–2445.
7. (a) P. Kumar, Y. M. Lee, L. Hu, J. Chen, Y. J. Park, J. Yao and W. Nam, *J. Am. Chem. Soc.*, **2016**, *138*, 7753–7762;

   (b) K. Gogoi, S. Saha, B. Mondal, H. Deka, S. Ghosh and B. Mondal, *Inorg. Chem.*, **2017**, *56*, 14438–14445;

   (c) H. Deka, S. Ghosh, S. Saha, K. Gogoi and B. Mondal, *Dalton Trans.*, **2016**, *45*, 10979–10988;

   (d) P. Kumar, Y. M. Lee, Y. J. Park, M. A. Siegler, K. D. Karlin and W. Nam, *J. Am. Chem. Soc.*, **2015**, *137*, 4284–4287.
8. M. A. Rhine, A. V. Rodrigues, R. J. Bieber Urbauer, J. L. Urbauer, T. L. Stemmler and T. C. Harrop, *J. Am. Chem. Soc*., **2014**, *136*, 12560–12563.
9. S. Saha, S. Maity, R. Mazumdar, B. Samanta, R. Ghosh, A. Guha and B. Mondal, *Inorg. Chem.,* **2023**, *62*, 17074–17082.